

Copyright
By
Juan José Icaza Aguirre
2004

**Factors Affecting Friction Losses in Multi-Strand Post-Tensioning
Tendons Including the Effect of Emulsifiable Oils**

by

Juan José Icaza Aguirre, B.S.C.E.

Thesis

Presented to the Faculty of the Graduate School of

The University of Texas at Austin

in Partial Fulfillment

of the Requirements

for the Degree of

Master of Science in Engineering

The University of Texas at Austin

August 2004

**Factors Affecting Friction Losses in Multi-Strand Post-Tensioning
Tendons Including the Effect of Emulsifiable Oils**

**APPROVED BY
SUPERVISING COMMITTEE:**

John E. Breen, Supervisor

Sharon L. Wood

To my parents

Acknowledgements

I would like to thank Dr. John E. Breen. It has been an honor to work with him. His advice is of great value to me. I would also like to thank Dr. Michael E. Kreger for his help in the initial stages of this investigation. He encouraged me, along with Dr. Eric B. Williamson, to pursue graduate studies.

The Texas Department of Transportation and the Federal Highway Administration sponsored the experimental research presented in this thesis. Their financial support is appreciated.

I would like to acknowledge the assistance of the administrative and technical staff of the Ferguson Structural Engineering Laboratory, especially Hortensia Peoples, Regina Forward, Mary Joe Moore, Blake Stasney, Dennis Phillip, and Mike Bell.

I thank my friends in Austin for their support throughout my graduate and undergraduate studies. My friends at the Ferguson Structural Engineering Laboratory deserve special mention. Christin Coselli, Jeff Diephuis, Tanya Luthi, and Mike Brown contributed to this work. Their friendship and help is appreciated very much.

I would also like to thank Don Filadelfo Chamorro for his advice and the many useful books he has given to me.

I want to express especial thanks to my uncle Salvador and my aunt Nina for their love and support throughout these years. With them I always felt at

home. I also want to thank my parents for their encouragement and example, and to my brothers, Alejo and Roberto.

Juan José Icaza

August 2004

Factors Affecting Friction Losses in Multi-Strand Post-Tensioning Tendons Including the Effect of Emulsifiable Oils

Juan José Icaza Aguirre, M.S.E.

The University of Texas at Austin, 2004

SUPERVISOR: John E. Breen

Emulsifiable oils are sometimes used in post-tensioned construction to provide temporary corrosion protection to the tendons in the period between stressing and grouting. It has been common practice to flush tendons with water to remove the oil, and then use compressed air to remove the water from the ducts. Often environmental concerns make disposal of the flushed oils difficult and costly. In addition, significant voids, pockets of water, and corroded strands have been found. It is believed that flushing with water and compressed air does not completely remove either the oil or the water, and such a practice is now strongly discouraged. Leaving the oil will certainly affect the bond strength of the tendon

and that can be a negative effect. However, previous research has shown that emulsifiable oils reduce the friction losses and this can be a positive effect. The objective of this research is to quantify the effects of lubrication with emulsifiable oils on the friction losses of multi-strand tendons. In addition, the effects of curvature, duct material, and the time between lubrication and stressing were investigated. Damage to the inside of the duct caused by stressing of the tendon was also studied.

Large-scale friction tests were performed using multi-strand tendons in three different conditions: dry (unlubricated), freshly oiled, and one day after oiling. These tests were performed with three different duct materials: steel pipe, corrugated galvanized steel duct, and high density polyethylene (HDPE) duct. The tests were repeated using two different radii of curvature.

Results from these tests indicated that the coefficient of friction was independent of the radius of curvature. However, different coefficients of friction were found for each duct material. The coefficient of friction found for steel pipes and galvanized steel ducts agree with those recommended in the literature. This was not the case for HDPE ducts. In this case the coefficient found was substantially lower than that recommended. Lubrication of the tendons reduced the coefficient of friction. However, this reduction was sometimes eliminated if a one day delay occurred between oiling and stressing. No significant damage was observed in either HDPE ducts or galvanized steel ducts.

Table of Contents

CHAPTER 1 INTRODUCTION.....	1
1.1 Background.....	1
1.2 Introduction to TxDOT Project 4562	3
1.3 Objectives	5
1.4 Scope	6
CHAPTER 2 BACKGROUND INFORMATION AND LITERATURE REVIEW	7
2.1 Introduction.....	7
2.2 Friction Losses in Post-Tensioned Concrete	8
2.3 Previous Research.....	11
2.3.1 Small-Scale Tests by Owens and Moore.....	12
2.3.2 NCHRP Project 4-15.....	13
2.3.3 Previous Research at Ferguson Structural Engineering Laboratory (TxDOT Project 1264)	14
2.4 Limitations of Previous Research.....	18
CHAPTER 3 EXPERIMENTAL PROGRAM.....	20
3.1 Introduction.....	20
3.1.1 Objectives	20
3.1.2 Selection of Emulsifiable Oils	20
3.1.3 Experimental Setup	21
3.2 Test Variables	23
3.3 Experimental Details	25
3.3.1 Specimens	25
3.3.2 Materials	30

3.4	Procedure	32
3.4.1	Casting of Specimens	32
3.4.2	Preparation for Test	37
3.4.3	Test Sequence	43
3.4.4	Removal of Replaceable Part	44
3.4.5	Determination of Hardware Losses	46
CHAPTER 4 TEST RESULTS		48
4.1	Friction Test Results	48
4.1.1	Steel Pipe	50
4.1.2	HDPE Duct.....	54
4.1.3	Galvanized Steel Duct	57
4.1.4	Hardware Losses	60
4.2	Damage to the Post-Tensioning Ducts	63
CHAPTER 5 EVALUATIONS OF TEST RESULTS		69
5.1	Introduction	69
5.2	The Effect of Curvature and Duct Material.....	72
5.3	The Effect of Lubrication.....	75
5.4	Comparison to Design Values and Recommendations	78
5.5	Significance of Findings	80
5.6	Summary.....	84
CHAPTER 6 SUMMARY AND CONCLUSIONS.....		86
6.1	Summary.....	86
6.2	Conclusions	87
6.3	Recommendations for Future Research.....	88

REFERENCES 89

VITA 92

List of Tables

Table 2-1 Friction and wobble coefficients (ACI 318-02).....	10
Table 2-2 Friction and wobble coefficients (AASHTO 1999, 2002).....	11
Table 2-3 Friction and wobble coefficients (PTI 1990)	11
Table 2-4 Friction tests performed by Owens and Moore (CIRIA 1978)	13
Table 2-5 Friction test results from NCHRP Project 4-15	14
Table 2-6 Results from small-scale friction tests (Kittleman et al 1993).....	16
Table 2-7 Results from large-scale tests by Davis and Tran (Davis et al 1993)...	18
Table 3-1 Experimental matrix and number of tests	25
Table 4-1 Specimen name scheme	48
Table 5-1 Average Percent Load Loss	70
Table 5-2 Average percent load loss due to curvature friction.....	71
Table 5-3 Average Friction Coefficient	72
Table 5-4 Comparison of friction coefficients to recommended values	79
Table 5-5 Reduction in friction coefficients compared to previous research.....	80

List of Figures

Figure 1-1 Schematic of deviators in the Long Key Bridge (Carter 1987).....	2
Figure 2-1 Wobble friction losses (Collins and Mitchell 1997).....	8
Figure 2-2 Curvature Friction Losses (Collins and Mitchell 1997).....	9
Figure 2-3 Test Setup used by Owen and Moore (CIRIA 1978).....	12
Figure 2-4 Test setup used by Hamilton and Davis (Kittleman et al 1993).....	15
Figure 2-5 Beam used by Tran and Davis (Tran 1993).....	17
Figure 3-1 Small-scale bond and accelerated corrosion test results.....	21
Figure 3-2 Placement of duct and casting of removable part.....	22
Figure 3-3 Test setup and removal of replaceable part.....	23
Figure 3-4 Cross-section details of permanent part of beam.....	26
Figure 3-5 Completed cross-section.....	27
Figure 3-6 Plan view of beams.....	29
Figure 3-7 Ducts.....	31
Figure 3-8 Completed forms for permanent part.....	32
Figure 3-9 Forms for permanent part during construction.....	33
Figure 3-10 Installation of steel pipe.....	35
Figure 3-11 Installation of HDPE duct.....	35
Figure 3-12 Installation of galvanized steel duct.....	36
Figure 3-13 Forms for replaceable part.....	36
Figure 3-14 Completed cross-section.....	37
Figure 3-15 Hydro-stone on face of beam.....	39
Figure 3-16 Dead end detail.....	40
Figure 3-17 Live end detail.....	41
Figure 3-18 Split rings on dead end.....	42
Figure 3-19 Oiling of tendon.....	43
Figure 3-20 Separation of permanent and replaceable part.....	45

Figure 3-21 Removing replaceable part	46
Figure 3-22 Determination of hardware losses	47
Figure 4-1 Specimen 1-SP-30°	50
Figure 4-2 Specimen 2-SP-30°	51
Figure 4-3 Specimen 0-SP-90°	52
Figure 4-4 Specimen 1-SP-90°	53
Figure 4-5 Specimen 2-SP-90°	53
Figure 4-6 Specimen 1-HD-30°	54
Figure 4-7 Specimen 2-HD-30°	55
Figure 4-8 Sharp bend on strand	56
Figure 4-9 Specimen 1-HD-90°	56
Figure 4-10 Specimen 2-HD-90°	57
Figure 4-11 Specimen 1-GD-30°	58
Figure 4-12 Specimen 2-GD-30°	58
Figure 4-13 Specimen 1-GD-90°	59
Figure 4-14 Specimen 2-GD-90°	60
Figure 4-15 Hardware losses - oil NC205	61
Figure 4-16 Hardware losses - oil 703D	62
Figure 4-17 Damage in specimen 1-HD-30°	63
Figure 4-18 Damage in specimen 2-HD-30°	64
Figure 4-19 Damage in specimen 1-HD-90°	65
Figure 4-20 Damage in specimen 2-HD-90°	65
Figure 4-21 Damage in specimen 1-GD-30°	66
Figure 4-22 Damage in specimen 1-GD-90°	66
Figure 4-23 Damage in specimen 2-GD-30°	67
Figure 4-24 Damage in specimen 2-GD-90°	67
Figure 5-1 Load loss due to curvature friction on Dry tests	73
Figure 5-2 Friction Coefficients on Dry tests	73

Figure 5-3 Average load loss on Dry tests	74
Figure 5-4 Average friction coefficients on Dry tests.....	75
Figure 5-5 Effect of fresh lubrication.....	76
Figure 5-6 Effect of lubrication one day after oiling.....	77
Figure 5-7 Results from Freshly Oiled and One Day After Oiling tests.....	78
Figure 5-8 Relationship between total angle change, coefficient of friction and percent load loss	82
Figure 5-9 Example of friction loss calculations (Collins and Mitchell 1997)	83

CHAPTER 1

Introduction

1.1 BACKGROUND

In 1928 Eugene Freyssinet began to use high-strength steel wires for prestressing concrete. Today more than 50% of bridges are constructed of prestressed concrete (Collins and Mitchells 1997). In prestressed concrete members, high-strength steel is pretensioned or post-tensioned against the concrete, causing compressive stresses in the concrete. Concrete is strong in compression but weak in tension. By precompressing the concrete, any tensile stresses caused by loading of the member are counter-acted by the compressive stress present previous to loading, making the prestressed member equally strong as the regularly reinforced concrete member, but significantly stiffer by preventing cracking of the concrete due to the elimination of tensile stresses.

There are two different types of prestressed concrete: pretensioned and post-tensioned. In pretensioned concrete, the steel wires or strands are stressed prior to casting concrete. Once the concrete is cast and cured, the strands are released, transferring the stresses to the concrete by bond. In post-tensioned concrete, the concrete members are cast with ducts where the steel strands will be placed after the concrete has hardened and cured. At this point the strands, usually called tendons, are stressed against the concrete member and the load is transferred at the ends by anchorages. Once the tendons have been anchored, the ducts are usually filled with grout, which bonds the tendon to the concrete and is called a bonded tendon. On the other hand, the tendons are called unbonded if the ducts are not grouted or if they are filled with grease. Post-tensioned members may also have external tendons, where the tendons are external to the cross-

section of the concrete member. External tendons are attached to the concrete member at the ends and sometimes at deviators blocks, where they change direction; in this case they are partially bonded tendons, otherwise external tendons are unbonded tendons.

Tendons in post-tensioned concrete are usually deviated or curved. For internal tendons this means that ducts where the tendons are contained curve along the length of the member. For external tendons, special deviator blocks through which the tendon passes are used to change the direction at discrete points. A schematic of a deviated tendon in a trapezoidal box girder is shown in Figure 1-1.

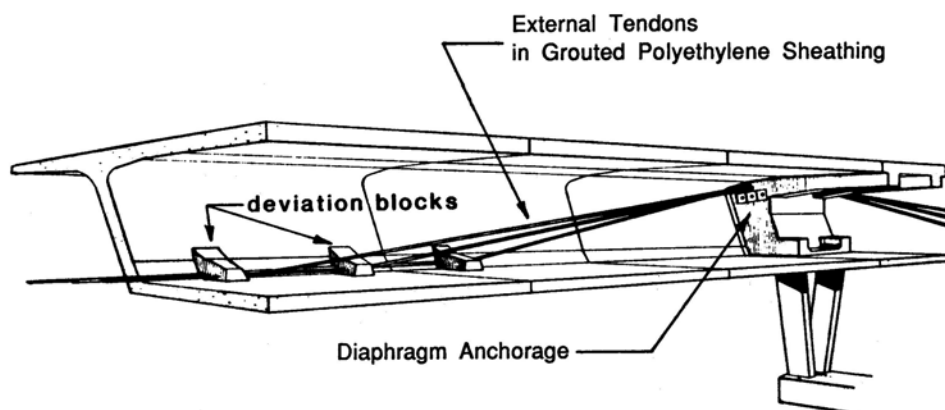


Figure 1-1 Schematic of deviators in the Long Key Bridge (Carter 1987)

Curved or deviated tendons are used to achieve more efficient designs. In negative moment regions of a continuous beam where the applied loads cause tension in the top and compression in the bottom, the tendon needs to be in the top to counteract the tensile stresses there, and not in the bottom where the loads cause compression. The opposite is true in positive moment regions. Curved tendons also occur in horizontally curved members.

Post-tensioned members may also be either monolithic or segmental. Monolithic members are cast entirely at once. In segmental construction, the member is divided into segments. Each segment is cast individually and sequentially. Therefore, the previously cast segment is used as a form for the adjacent segment. This technique is called match casting. Match casting ensures proper fitting of adjacent segments when they are joined. The segments are joined and then the tendons are installed and post-tensioned. The trapezoidal box girder shown in Figure 1-1 is a segmental girder.

Early attempts to create prestressed concrete members were unsuccessful due to loss of prestress. Losses in pretensioned members are due to elastic shortening of the concrete, shortening of the concrete due to shrinkage and creep, and to relaxation of the steel. Losses in post-tensioned concrete are due to shortening of the concrete due to shrinkage and creep, relaxation of the steel, friction along the length of the tendon, and losses at the anchorages, both due to friction and to seating.

Successful prestressed members were achieved by using both high-strength steel and concrete. High-strength steel allowed for higher levels of prestress so that even after losses significant amounts of prestress remained. Today the most commonly used form of steel reinforcement for prestressed concrete is the seven-wire strand, with a tensile strength of 270 ksi. High-strength concrete reduces the losses due to shrinkage and creep.

1.2 INTRODUCTION TO TXDOT PROJECT 4562

The use of post-tensioned structures has increased tremendously in the last 50 years. Although most structures have performed excellent throughout their design life, recently several corroded tendons were discovered in U.S. bridges. In 1999 one of the external tendons in the Niles Channel Bridge, built in 1983, failed

due to corrosion at an expansion joint (Freyermuth 2001). In 2000 several corroded tendons were discovered in the segmental piers of the Sunshine Skyway Bridge, built in 1986 (Poston and West 2001).

Durability concerns led the Texas Department of Transportation (TxDOT) to fund Project 1405 to study the overall durability of post-tensioned structures (Salas 2003). Specifically, the project studied the corrosion in internal post-tensioning tendons. However, the focus of project 1405 was long-term durability. There is concern that corrosion of the post-tensioning tendon may start before grouting.

Emulsifiable oils are sometimes used in post-tensioned construction to provide temporary corrosion protection to the tendons in the period between stressing and grouting. It has been common practice to flush tendons with water to remove the oil, and then use compressed air to remove the water from the ducts. Often environmental concerns make disposal of the flushed oils difficult and costly. In addition, significant voids, pockets of water, and corroded strands have been found. It is believed that flushing with water and compressed air does not completely remove either the oil or the water, and such a practice is now strongly discouraged. Leaving the oil will certainly affect the bond strength of the tendon and that can be a negative effect. However, previous research (Kittleman et al. 1993) has shown that emulsifiable oils reduce the friction losses and this can be a positive effect. Quantification of these effects with full-size tendons tests is highly desirable.

TxDOT Project 4562 is a result of these concerns. It is divided in two phases. The first phase will identify oils that could provide temporary corrosion protection in post-tensioning tendons, study the effect of the oils on friction losses and on the bond in multi-strand tendons, and investigate how flexural capacity is

affected by the loss of bond. The second phase will investigate the use of alternate corrosion-resistant post-tensioning systems.

Phase one is divided into seven tasks:

1. Identification of emulsifiable oils
2. Accelerated corrosion testing
3. PTI/ASTM strand pullout tests
4. Large-scale tendon friction tests
5. Large-scale bond tests
6. Development of specification and code changes
7. Preparation of reports

Tasks one through three have been performed at the Pennsylvania State University by Salcedo (2003) under the supervision of Dr. Andrea Schokker, who was involved in TxDOT project 1405 (Salas 2003). Tasks four through seven and phase two are being conducted at the Ferguson Structural Engineering Laboratory of the University of Texas at Austin under the supervision of Dr. John Breen. This report concerns only task four. Task five was performed simultaneously with task four and is reported by Diephuis (2004).

1.3 OBJECTIVES

The objectives of TxDOT project 4562 were stated earlier. This report deals exclusively with task four of phase one of the project. The primary objective is to quantify the reduction of friction losses in multi-strand tendons due to lubrication with emulsifiable oils. Both freshly oiled and previously oiled tendons need examination. The secondary objective is to study the effects on friction losses of curvature and duct material. In addition, the damage to the inside of the ducts will be examined.

The overall goal of the project is to improve durability of post-tensioned members. Earlier tests have shown that plastic ducts are highly desirable. It is possible that costs of this material might be somewhat offset by reductions in friction losses allowing less strands to be used to produce a desired prestress force.

1.4 SCOPE

From the recommendations made by Salcedo (2003) from tasks one through three, two oils were selected for further study in large-scale specimens. Three duct materials were selected for examination. Chapter 2 gives background information on friction losses that includes theory, recommendations for design, and findings of previous research. A description of the rationale behind the selection of these two oils, and details of the tests procedures and specimens are found in Chapter 3. Chapter 4 presents the results from all tests, and reports the damage to the interior of the post-tensioning ducts due to bearing of the strands during stressing. Chapter 5 presents an analysis of the data, recommendations and practical implementation. Chapter 6 is a summary and gives conclusions.

CHAPTER 2

Background Information and Literature Review

2.1 INTRODUCTION

The ability to control the stresses is vital to prestressed concrete systems. Using different amounts and locations of prestress permits tailoring stresses to achieve the desired behavior. The advantage of prestressed concrete systems over conventionally reinforced concrete systems is precisely this ability to modify the stresses, and consequently the behavior, to meet the specific needs of the structure. Therefore, accurate predictions of the effective tendon force (prestress) are crucial in the design of prestressed concrete systems.

In post-tensioned systems, the effective tendon force will vary along the length of the tendon. Variations in the tendon forces are due to losses that occur both immediately after stressing and with time. Immediate losses include those at the anchorages (including seating losses) and losses along the length of tendon due to friction. Time-dependent losses include those due to creep of concrete, shrinkage of concrete, and steel relaxation.

Over-prediction of prestress losses will increase the size of the tendon required in order to compensate for the loss, leading to uneconomical designs. In addition, overstressing the concrete members may cause excessive camber and unexpected cracking. On the other hand, under-prediction of prestress losses will cause decreased stiffness (increase in deflections) that may lead to serviceability issues. If losses are very large, the behavior of the system will resemble that of a conventionally reinforced concrete system, losing all of the advantages of the prestressed system. Cracking will be possible under service loads. Cracking

allows for the ingress of water and chlorides that will undermine the durability of the system (Salas 2003) and can also lead to fatigue problems (Hagenberger 2004)

2.2 FRICTION LOSSES IN POST-TENSIONED CONCRETE

Friction losses in post-tensioned concrete systems consist of two components: losses due to the intentional curvature and losses due to unintentional angle changes along the tendon. The former is called curvature friction and the latter is called wobble friction (see Figure 2-1 and Figure 2-2). Curvature friction losses are proportional to tendon angle changes while the wobble friction losses are proportional to tendon length.

Wobble friction losses depend on the stiffness of the post-tensioning duct, its diameter, spacing of the duct supports, tendon type, duct type, and the quality of the workmanship (Collins and Mitchell 1997). Curvature friction losses depend on the coefficient of friction between the contact materials (the tendon and the duct), and the force exerted by the tendon on the duct.

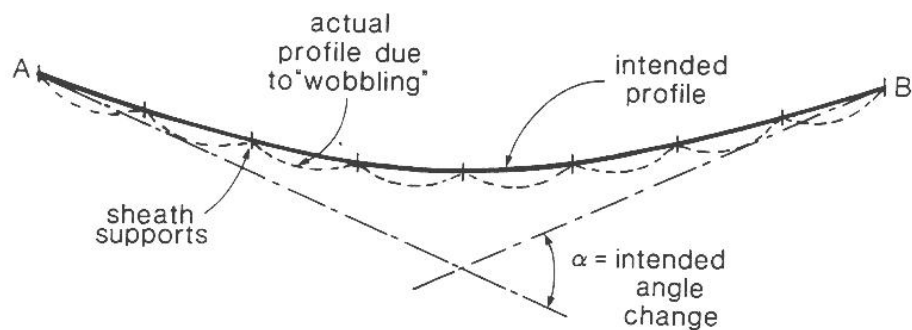


Figure 2-1 Wobble friction losses (Collins and Mitchell 1997)

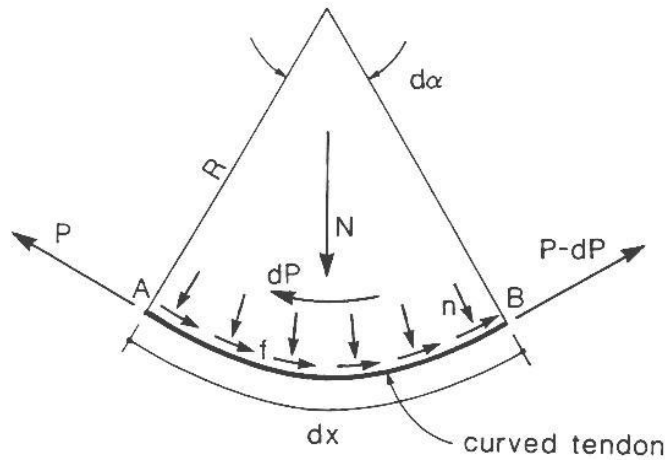


Figure 2-2 Curvature Friction Losses (Collins and Mitchell 1997)

Considering a curved tendon of infinitesimal length dx , whose radius of curvature is R , as show in Figure 2-2, then the angle change, $d\alpha$, is given by $d\alpha = \frac{dx}{R}$. Assuming that the normal force, N , along this infinitesimal length is constant, it can be shown that for small angles $d\alpha$, $N = Pd\alpha$. P is the force in the tendon.

The frictional force, dP , is equal to the normal force N times the coefficient of friction μ in the opposite direction of dP , $dP = -\mu N$. Substituting for N , gives $dP = -\mu Pd\alpha$, and solving for P gives $\frac{dP}{P} = -\mu d\alpha$.

Integration on both sides from point A (where the load is being applied) to point B (where tendon force is being computed) gives:

$$\int_{P_A}^{P_B} \frac{dP}{P} = \int_{P_A}^{P_B} -\mu d\alpha \quad \text{Equation 2-1}$$

$$\ln\left(\frac{P_B}{P_A}\right) = -\mu\alpha \quad \text{Equation 2-2}$$

$$\frac{P_B}{P_A} = e^{-\mu\alpha} \quad \text{Equation 2-3}$$

$$P_B = P_A e^{-\mu\alpha} \quad \text{Equation 2-4}$$

where P_A and P_B are the tendon forces at points A and B respectively. The above formula may also be used for computing wobble friction losses by substituting the term KL for $\mu\alpha$, where K is an empirical wobble coefficient in units of 1/length, and L is the length of the tendon from point A to B . Computation of friction losses due to both curvature and wobble friction yields the well known equation:

$$P_B = P_A e^{-(\mu\alpha+KL)} \quad \text{Equation 2-5}$$

Approximate values of μ and K are available in the literature and are based on experience. ACI 318-02 recommends in the commentary the values shown in Table 2-1. It also recommends ignoring wobble friction losses in rigid conduits and for large diameter prestressing steel in semi-rigid type conduit.

AASHTO's recommended values for the coefficients are shown in Table 2-2. These values appear in both the Standard Specification for Highway Bridges (AASHTO 2002) and in the Guide Specifications for Design and Construction of Segmental Concrete Bridges (AASHTO 1999).

Table 2-1 Friction and wobble coefficients (ACI 318-02)

			K (1/ft)	μ
Grouted tendons in metal sheathing		Wire tendons	0.0010-0.0015	0.15-0.25
		High-strength bars	0.0001-0.0006	0.08-0.30
		7-wire strand	0.0005-0.0020	0.15-0.25
Unbonded tendons	Mastic coated	Wire tendons	0.0010-0.0020	0.05-0.15
		7-wire strand	0.0010-0.0020	0.05-0.15
	Pre-greased	Wire tendons	0.0003-0.0020	0.05-0.15
		7-wire strand	0.0003-0.0020	0.05-0.15

Table 2-2 Friction and wobble coefficients (AASHTO 1999, 2002)

Type of Steel	Type of Duct	K (1/ft)	μ
Wire or strand	Rigid and semi-rigid galvanized metal sheathing	0.0002	0.15 – 0.25 ^a
	Polyethylene	0.0002	0.23
	Rigid steel pipe	0.0002	0.25 ^b
High strength bars	Galvanized metal sheathing	0.0002	0.15

^a A friction coefficient of 0.25 is appropriate for 12-strand tendons. A lower coefficient may be used for larger tendon and duct sizes.
^b Lubrication will probably be required.

Most values recommended by both ACI and AASHTO are in the form of ranges. This reflects the variability of friction coefficients in practice. The same is true for the values recommended by PTI, shown in Table 2-3.

Table 2-3 Friction and wobble coefficients (PTI 1990)

Type of Duct	Range of Values		Recommended for Calculations	
	μ	K (x 10 ⁻⁴ 1/ft)	μ	K (x 10 ⁻⁴ 1/ft)
Flexible tubing non-galvanized	0.18 – 0.26	5 – 10	0.22	7.5
Flexible tubing galvanized	0.14 – 0.22	3 – 7	0.18	5.0
Rigid thin wall tubing non-galvanized	0.20 – 0.30	1 – 5	0.25	3.0
Rigid thin wall tubing galvanized	0.16 – 0.24	0 – 4	0.20	2.0
Greased and wrapped	0.05 – 0.15	5 – 15	0.07	10.0

2.3 PREVIOUS RESEARCH

Emulsifiable oils have been used in the past to both temporarily protect tendons from corroding in the time between stressing and grouting and to reduce friction losses. However, none of these products are marketed specifically for this use (Kittleman 1992). This section summarizes the results of previous research on

the use of emulsifiable oils for reducing friction losses in post-tensioned concrete as well as research on friction coefficients used in different duct materials.

2.3.1 Small-Scale Tests by Owens and Moore

Owens and Moore conducted research (CIRIA 1978) to investigate the effect of different surface conditions on friction in post-tensioned tendons. The study used single-strand tendons of four different types: 7 mm wire, 12.7 mm drawn strand, 15.2 mm round wire strand, and 18 mm drawn strand. The three surface conditions investigated were clean, rusty, and oiled. The results of these small-scale tests are shown in Table 2-4.

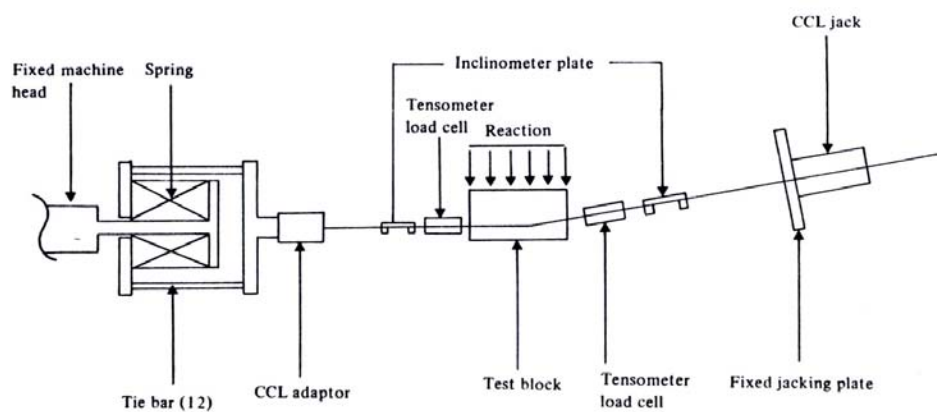


Figure 2-3 Test Setup used by Owen and Moore (CIRIA 1978)

The test setup used by Owen and Moore is shown in Figure 2-3. The procedure consisted in loading the tendon up to 80% of its breaking load in ten to fifteen increments. The results showed no significant decrease in friction in the oiled condition; they did show an increase in friction in the rusty condition (CIRIA 1978).

Table 2-4 Friction tests performed by Owens and Moore (CIRIA 1978)

Test No.	Tendon Type	Average Coefficient of Friction (μ)	Tendon Condition
1	7 mm wire	0.12	Clean
2		0.12	Clean
3		0.10	Clean
4		0.31	Rusty
5		0.26	Less rusty than 4
6		0.19	Less rusty than 5
24		0.09	Clean
25	0.11	Clean	
7	12.7 mm drawn strand	0.15	Clean
8		0.17	Clean
9		0.14	Clean
10		0.27	Rusty
11		0.35	Rusty
12		0.22	Rusty
13	15.2 mm round wire strand	0.16	Clean
14		0.14	Clean
15		0.17	Clean
16		0.15	Oiled
17		0.16	Oiled
18		0.16	Oiled
19		0.46	Rusty
20		0.31	Rusty
21		0.28	Rusty
22		18 mm drawn strand	0.19
23	0.17		Clean

2.3.2 NCHRP Project 4-15

The objective of NCHRP Project 4-15 was to evaluate the current practices in corrosion protection of prestressed bridges in the US and the effectiveness of the newer systems and materials available at the time (Perenchio et al 1989). The research project included an extensive literature review, accelerated corrosion tests, and mechanical tests of the newer systems and materials. These mechanical tests included friction tests in both galvanized steel ducts and in polyethylene ducts. However, no tests were performed using

lubricants even though emulsifiable oils were mentioned for temporary corrosion protection.

The test setup consisted of two sets of four ducts cast into a 14 in. thick concrete slab in the shape of a quarter circle with a radius of 15.25 ft. The ducts had nominal diameters of 2 in. The first set contained the galvanized steel ducts and the second set the polyethylene ducts. Within each set, two of the ducts were tested with bare strand, and the other two with epoxy coated strand. The tendons used 4 strands. The results from these friction tests are shown in Table 2-5. The table shows the average friction coefficients.

Table 2-5 Friction test results from NCHRP Project 4-15

Average Friction Coefficient	Bare Strand	Epoxy Coated Strand
Galvanized Metal Duct	0.23	0.40
Polyethylene Duct	0.18	0.205

2.3.3 Previous Research at Ferguson Structural Engineering Laboratory (TxDOT Project 1264)

The Texas Department of Transportation (TxDOT) in cooperation with the U.S. Department of Transportation, Federal Highway Administration sponsored a research project at the Ferguson Structural Engineering Laboratory to evaluate agents for lubrication and temporary corrosion protection of post-tensioning tendons (Kittleman et al. 1993) used both in monolithic and segmental construction (Davis et al. 1993).

That project identified ten emulsifiable oils as candidates for corrosion protection and lubrication. These ten oils were subjected to a series of small-scale corrosion, friction and adhesion tests (Kittleman et al. 1993). The overall performance of these ten oils was compared and four were recommended for further study in the large-scale tests.

The next two sub-sections report the findings of the friction tests of that study. The results of the small-scale friction tests performed by Hamilton and Davis (Davis 1993) are presented first. Then the results of the large-scale friction tests in monolithic and segmental girders performed by Tran and Davis (Tran 1992; Davis 1993), respectively, are given. All tests performed in this study used galvanized metal ducts and seven-wire, 0.5-in. strand.

2.3.3.1 *Small-Scale Tests by Hamilton and Davis*

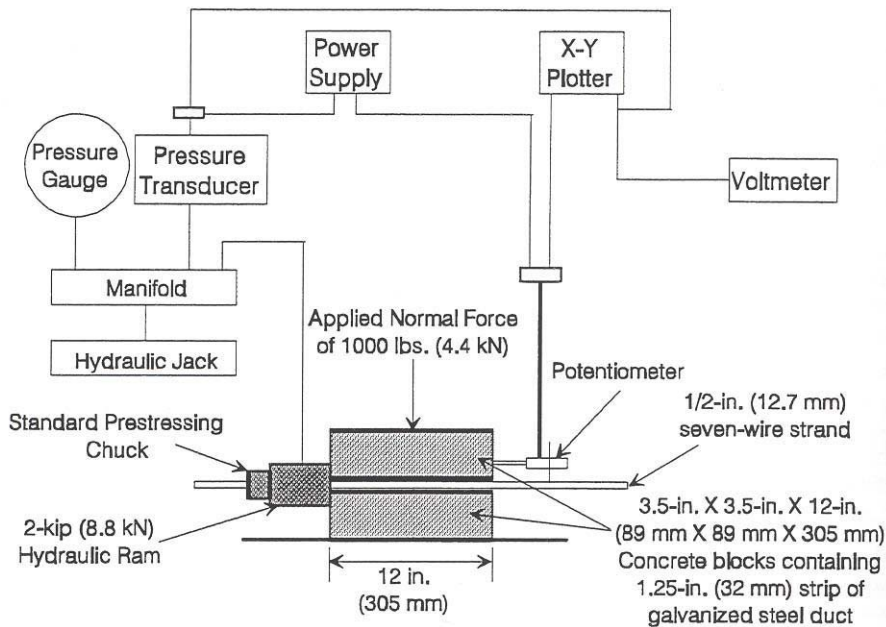


Figure 2-4 *Test setup used by Hamilton and Davis (Kittleman et al 1993)*

The test setup used is shown in Figure 2-4. Two one-ft long concrete blocks were pressed against each other. Between the blocks there were two strips of galvanized metal duct with a single strand placed between the two strips of ducts. The compressive force on the blocks was 1 kip. The strand is then pulled from one end. The force at which the strand started to move divided by the normal

force (1 kip) gave the coefficient of static friction. Similarly, the force at which the strand kept moving divided by the normal force gave the coefficient of dynamic friction. The same procedure was used for the lubricated strands.

The results of the static and dynamic friction tests for the ten lubricants are shown in Table 2-6. Values for the coefficient of static friction in the dry condition ranged from 0.22 to 0.30 and for the dynamic coefficient of friction ranged from 0.24 to 0.32. The four recommended oils for the large-scale tests were Texaco Soluble D, Wright 502, Dromus B, and Hocut 4284.

Table 2-6 Results from small-scale friction tests (Kittleman et al 1993)

Lubricant	Static Reduction in Friction	Dynamic Reduction in Friction
Visconorust 8415E	17%	6.1%
Dromus B*	17%	5.9%
Unocal 10	14%	6.0%
Unocal MS	14%	6.0%
Texaco Soluble D*	27%	14%
Rust-veto FB20	0%	-6.1%
Hocut 737	-9%	-6.3%
Hocut 4284*	18%	10%
Nalco 6667	12%	1.9%
Wright 502*	21%	14%
“-” indicates increase in friction due to lubricant.		
* indicates recommended oil for large-scale tests.		

2.3.3.2 Large-Scale Tests by Tran and Davis

The large scale tests performed by Tran (1992) were identical to those performed by Davis (1993). The only difference between the two was that those performed by Tran were built monolithically, while those by Davis were built segmentally. The specimens and procedures were otherwise the same.

The test setup consisted of a two 78-ft long concrete beams. One was built monolithically while the other segmentally. Each contained eight post-tensioning ducts. Two of these eight ducts were straight, while the others were parabolically curved. The total curvatures on the six ducts were identical. A schematic of the test beam and duct profiles is show in Figure 2-5.

The ducts were galvanized steel ducts with nominal diameter of 2.125 in. The tendons consisted of seven, ½-in., Grade 270, strands. Tendons were stressed up to 80% of their breaking strength in 20 kips increments during the first half of the loading, and at 10 kip increments during the last half.

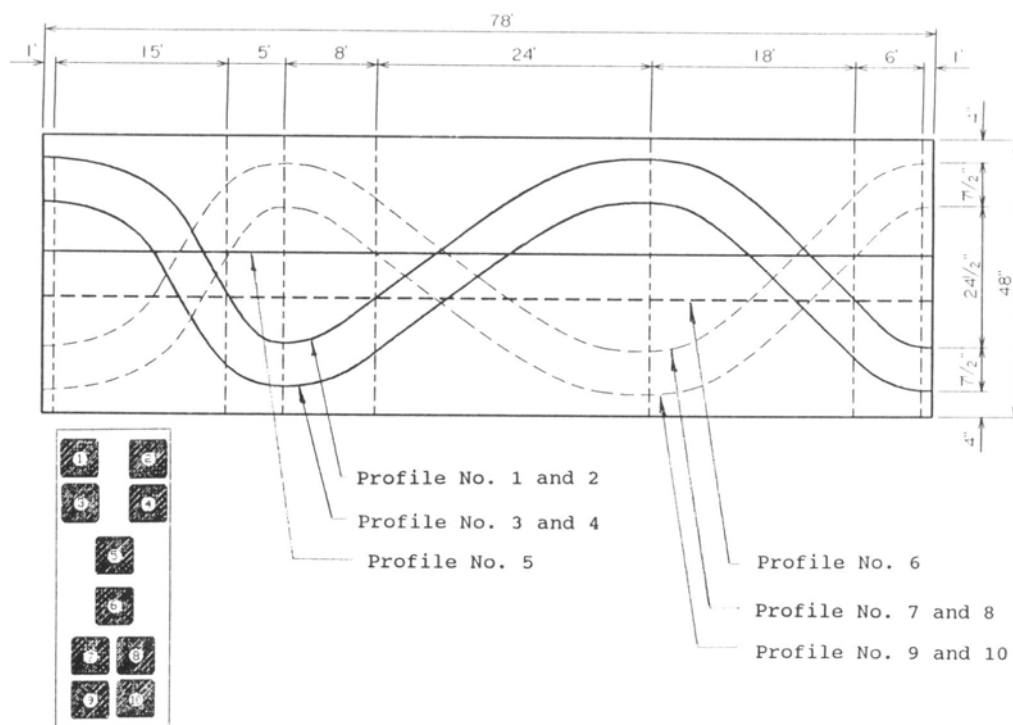


Figure 2-5 Beam used by Tran and Davis (Tran 1993)

The two straight ducts were used to determine the wobble coefficient for both the monolithic and segmental beam. The curved ducts were used to determine the friction coefficient for a bare tendon and for the lubricated tendons

with the four different emulsifiable oils recommended by Hamilton and Davis. However, in the segmental beam, only the lubricant Wright 502 was tested, because the emphasis of the tests was to compare it to the monolithic tests. Table 2-7 shows the reduction in friction due to lubrication with each of the four different oils. The tests performed on the bare tendons showed an average coefficient of friction of 0.153.

Table 2-7 Results from large-scale tests by Davis and Tran (Davis et al 1993)

Lubricant	Reduction in Friction Coefficient	
	Monolithic Beam	Segmental Beam
Texaco Soluble D	19%	-
Wright 502	25%	15%
Hocut 4284	17%	-
Dromus B	8%	-

2.4 LIMITATIONS OF PREVIOUS RESEARCH

Friction coefficients recommended by ACI, AASHTO and PTI are the result of extensive experience and research. The previous section showed that in general, friction coefficients for 7-wire strand tendons on galvanized steel duct are in the range of 0.15 to 0.25.

However, the need for research is still great. There is little research on friction in polyethylene ducts. Although some research has been conducted on the effect of emulsifiable oils on friction, most of it has been with galvanized steel ducts. In addition, because the emulsifiable oils have not been marketed for this use, many different oils have been used. Previous research on the use of emulsifiable oils was carried out using oils that are not used or no longer available commercially.

This experimental study will explore the following areas:

1. The reduction in friction in galvanized steel ducts, polyethylene ducts, and steel pipe due to lubrication with emulsifiable oils currently available commercially.
2. Friction losses in polyethylene ducts without lubrication.
3. The effect of curvature on the friction coefficient.

CHAPTER 3

Experimental Program

3.1 INTRODUCTION

3.1.1 Objectives

The primary objective of this experimental study is to determine the reduction in friction losses in post-tensioned concrete members produced by lubrication of the tendons with emulsifiable oils. The secondary objective of this study is to investigate the effect of the following factors on friction losses:

1. Duct material
2. Curvature
3. Time between application of oil and stressing of tendon.

3.1.2 Selection of Emulsifiable Oils

As explained previously, these friction tests were part of a larger study of the effects of emulsifiable oils used as temporary corrosion protection in grouted post-tensioned tendons. This larger study included accelerated corrosion tests and small scale bond tests done by Salcedo (2003). In addition, large-scale bond tests were performed by Diephuis (2004) simultaneously with the friction tests reported in this thesis.

The same oils were used in these friction tests and in the large scale bond tests performed by Diephuis. Because of the laborious and time-consuming nature of these large-scale tests (both friction and bond), only two oils could be tested.

Nineteen oils were used in the accelerated corrosion and small-scale bond tests performed by Salcedo. Salcedo's results from both the small-scale bond and accelerated corrosion tests are shown in Figure 3-1. The figure only shows the

bond test results of the seven oils that received satisfactory performance rating (below a rating of 4.0) in the accelerated corrosion tests.

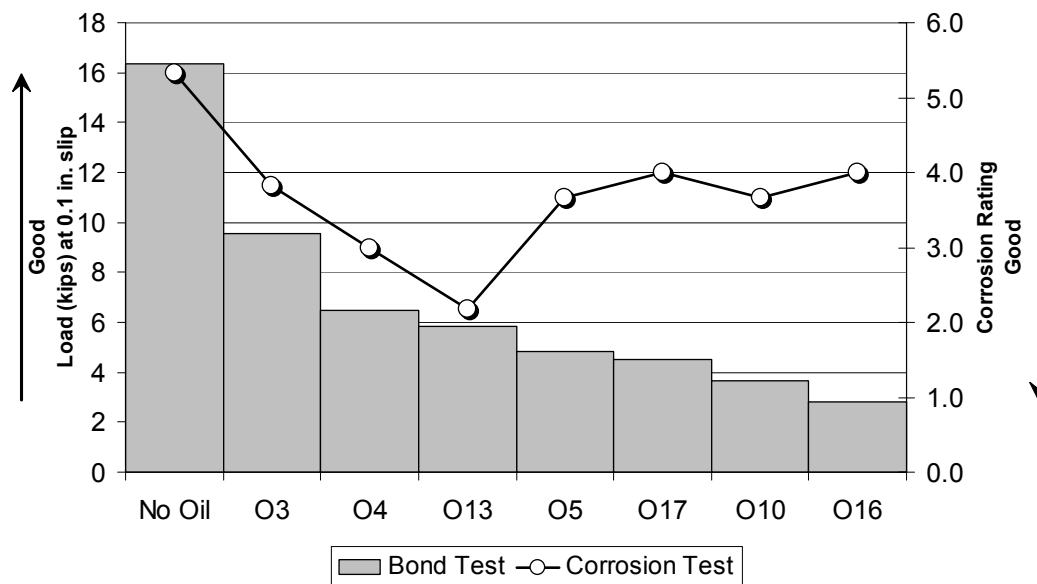


Figure 3-1 Small-scale bond and accelerated corrosion test results

The oil that performed the best in the bond tests, of these seven, was O3 (TRUKUT® NC205), and the worst was O16. Because these oils were also going to be used for the large-scale bond tests carried out by Diephuis, O3 and O16 were initially selected for testing to provide an upper and lower bound on bond behavior. However, because O10 performed somewhat similarly to O16 in the small-scale bond test, but had a somewhat better performance in the accelerated corrosion tests, O10 (Nox-Rust® 703D) was used instead of O16. For consistency with the large scale bond tests, the same oils were used in the friction tests.

3.1.3 Experimental Setup

The original idea for the test setup was taken from similar tests done in Germany (Cordes, Schütt, and Trost 1981). However, their setup was modified to

accommodate the larger scale of these tests. All tests used twelve, 0.5-in. strand tendons.

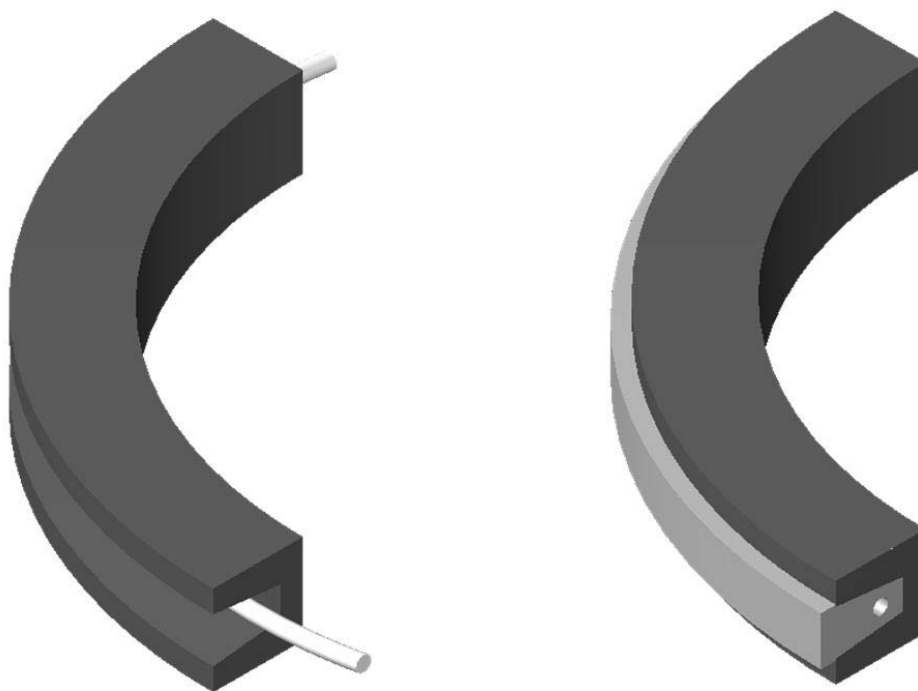


Figure 3-2 Placement of duct and casting of removable part

The setup was rather simple: a post-tensioning duct was embedded in a cavity of a curved concrete beam (dark shading in Figure 3-2). Infill concrete was then cast around the duct (lighter shading in Figure 3-2). The tendon was then fed through the duct and stressed using a hydraulic ram at one end (live end) and an anchor at the other end (dead end). Forces were measured with a pressure transducer at the live end, and with load cells at the dead end. The difference in force between the two ends is the friction loss caused by the tendon sliding against the inner wall of the curved post-tensioning duct.

In order to test the large numbers of specimens, the curved beam was designed in two parts, the permanent reaction beam and the replaceable cavity

infill that contained the post-tensioning duct. Further details of the specimens are given in Section 3.3. Figure 3-2 shows the permanent part with the post-tensioning duct ready for and after casting the replaceable part. While Figure 3-3 shows the test setup and removal of the replaceable part after testing.

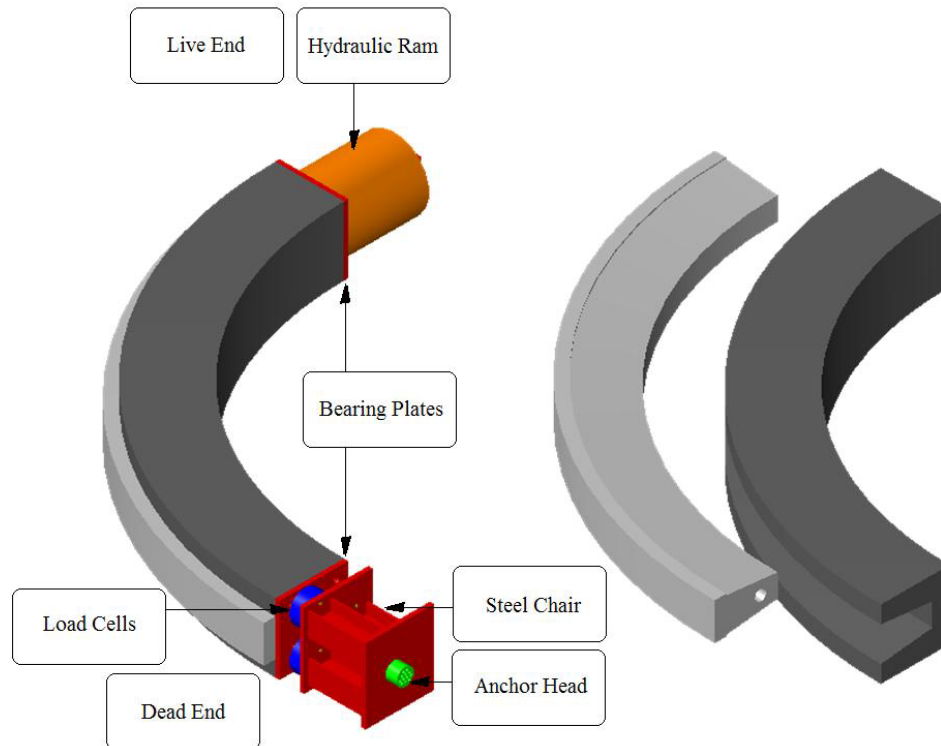


Figure 3-3 Test setup and removal of replaceable part

3.2 TEST VARIABLES

To accomplish the primary objective of this study, friction losses were determined for three different tendon conditions: no lubrication (dry condition), lubrication with emulsifiable oil with stressing immediately after application of the oil, and lubrication with emulsifiable oil but in a dry condition by delaying stressing for a day after application of the oil.

The third condition was added to this experimental program in response to observations (Salcedo, 2003) that oils dry rapidly over time and that reduction in friction losses could be significantly different after the oil had dried.

Tests were performed using three different duct materials: rigid galvanized steel pipe, semi-rigid corrugated galvanized steel duct, and high density polyethylene (HDPE) duct. Steel pipes are commonly used for anchor blisters or in deviator blocks where large angle changes are concentrated over small distances. In post-tensioned beams, corrugated galvanized steel duct has been the industry standard for many years. However, due to durability concerns in post-tensioned concrete structures, the use of plastic ducts is now recommended (Salas, 2003), and its use will probably increase in the future.

In addition, all of the above mentioned tests were performed using two beams with different radius of curvature. One had a radius of 10 ft and one had a radius of 30 ft. The beams were identical in length, cross-section, and reinforcement.

Both the Standard Specification for Highway Bridges (AASHTO 2002) and the Guide Specifications for Design and Construction of Segmental Concrete Bridges (AASHTO 1999) establish 30 ft as the minimum radius of curvature for HDPE ducts and 10 ft as the minimum for all other materials. These two radii were chosen for this experiment to reflect the lower bound of radius of curvature, and consequently the upper bound of friction losses. Although the 10-ft radius of curvature is not currently allowed for HDPE ducts, tests were performed using this radius for both comparison purposes and to investigate the performance of this material at this curvature.

All of the experimental variables and the number of tests are shown in Table 3-1. Each specimen is represented as a line in the table. Therefore, 7 tests were performed on each specimen.

Table 3-1 Experimental matrix and number of tests

Duct Material	Oil	Radius of Curvature	Condition		
			Dry	Oiled, tested immediately	Oiled, tested one day later
Galvanized Steel Pipe	NC 205	10 ft	3	2	2
		30 ft	3	2	2
	703D	10 ft	3	2	2
		30 ft	3	2	2
HDPE Duct	NC 205	10 ft	3	2	2
		30 ft	3	2	2
	703D	10 ft	3	2	2
		30 ft	3	2	2
Galvanized Steel duct	NC 205	10 ft	3	2	2
		30 ft	3	2	2
	703D	10 ft	3	2	2
		30 ft	3	2	2

3.3 EXPERIMENTAL DETAILS

3.3.1 Specimens

A beam in which the post-tensioning duct could be replaced was designed. The beam consisted of two parts: a replaceable infill that contained the post-tensioning duct, and a permanent one that was reused. The cross-sectional details of the permanent part are shown in Figure 3-4, and the completed section is shown in Figure 3-5. Bond between the two sections was prevented by the use of a concrete debonder to allow easy removal of the infill section after testing.

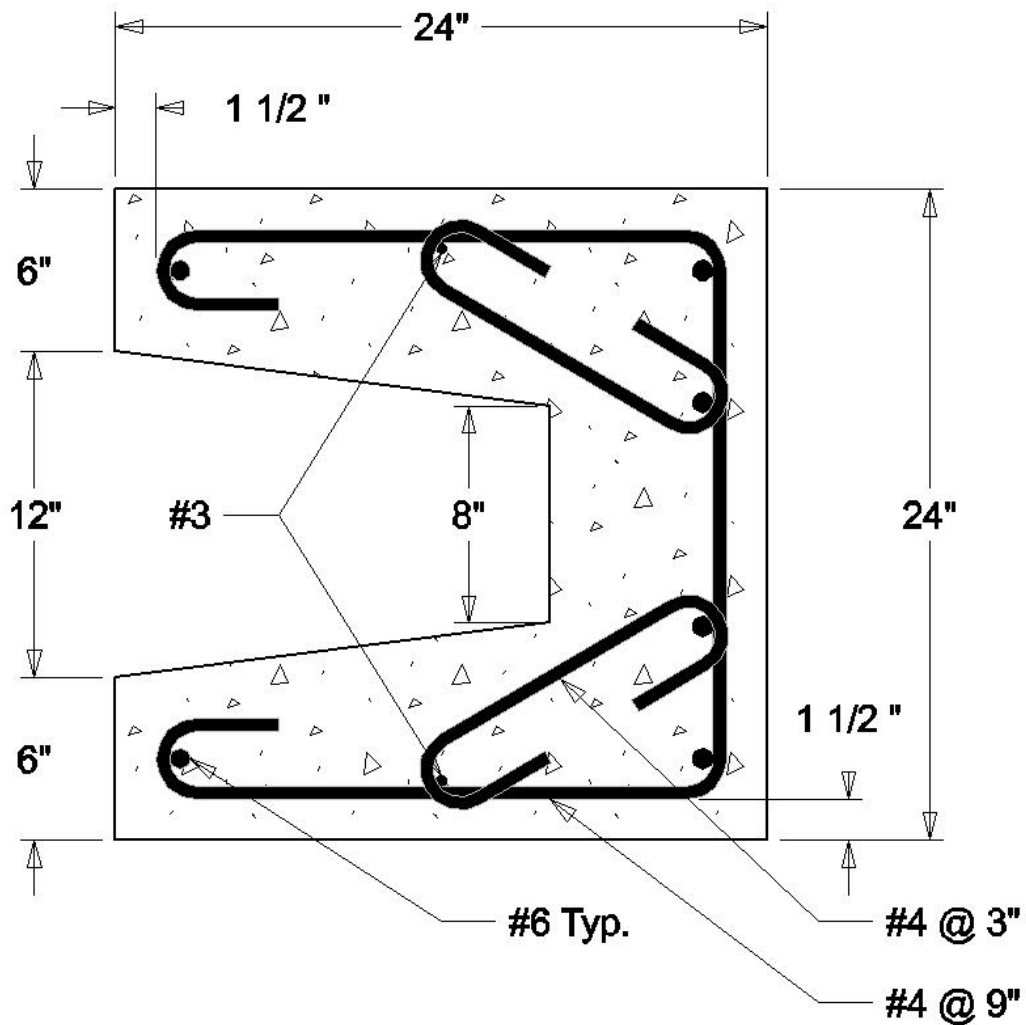


Figure 3-4 Cross-section details of permanent part of beam

The permanent part consisted of a C-shaped cross-section 24 in. wide and 24 in. tall. It was designed to carry the full compression load caused by post-tensioning of the tendon. Diagonal ties were added to prevent cracking caused by the radial forces created during post-tensioning. In addition, it had enough reinforcement so that the beam could be lifted and would have enough capacity to take any moment due to incidental eccentricities in post-tensioning. Therefore, post-tensioning of the beam did not require any reinforcement in the replaceable

part. However, it was expected that when galvanized steel duct or HDPE ducts were used, some reinforcement would be necessary to prevent cracking of the replaceable part during separation or lifting during removal.

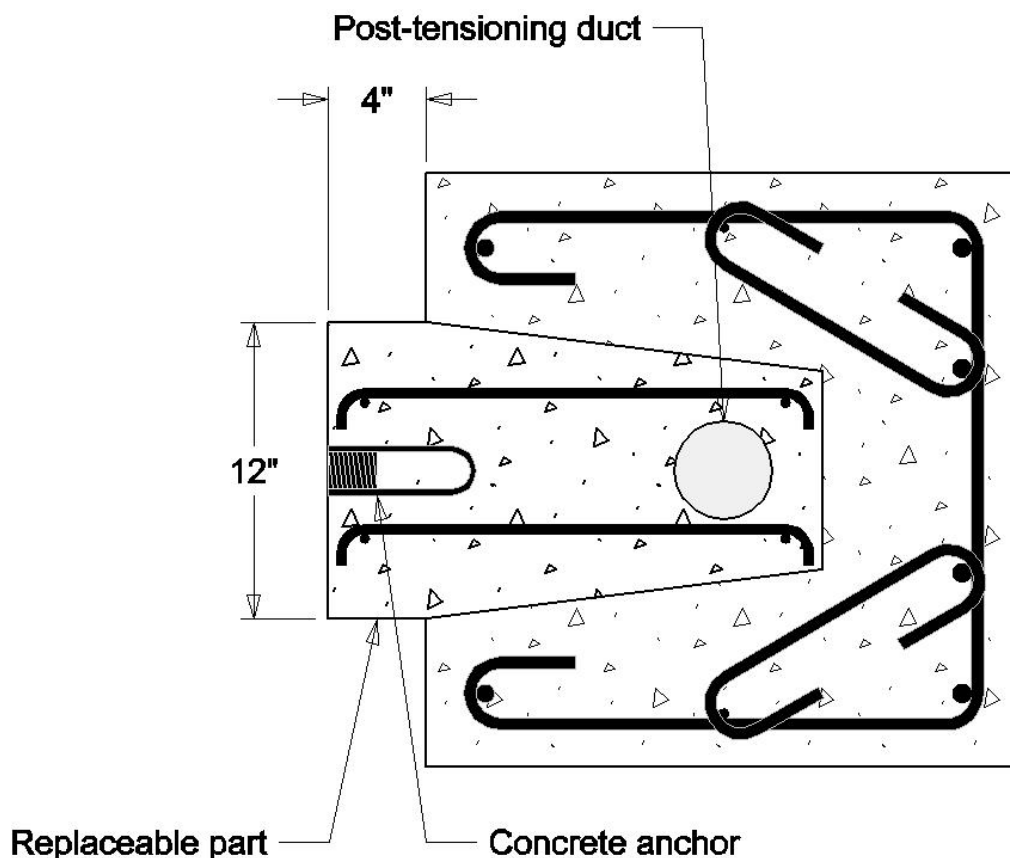


Figure 3-5 Completed cross-section

The replaceable part was not reinforced in the first three sets of specimens when steel pipes were used as the post-tensioning duct. However, cracking of the replaceable part occurred during separation of the last specimen with steel pipe. Therefore, for the rest of the specimens, where HDPE ducts or galvanized steel ducts were used, the replaceable part was lightly reinforced with two #3 transverse ties spaced at approximately 24 in. and four #3 bars as longitudinal

reinforcement, as shown in Figure 3-5. This reinforcement allowed the replaceable part to be lifted safely and prevented cracking during separation.

The replaceable part contained a concrete anchor used in the separation process. The tapered shape of the replaceable part was intended to provide easy separation of the two parts. The duct was placed in a position that would coincide with the center of the 24-in. square of the permanent part. The 4-in. extension, beyond the 24-in. square, was needed for casting concrete from the side.

Two of the permanent beams were built. They had identical cross-sections and centerline lengths, but they had different curvatures. As shown in Figure 3-6, one beam had a radius of curvature of 30 feet and total angle change of 90 degrees, while the other had a radius of curvature of 10 feet and a total angle change of 30 degrees. Centerline length of both beams was 188.5 in.

Neither of the two beams had any special details at the ends for post-tensioning. Steel bearing plates were used at the ends to attach the hydraulic equipment and the anchors. This setup allowed for the reuse of the post-tensioning anchor heads and eliminated the need for trumpets and spiral reinforcement at the ends of the beams.

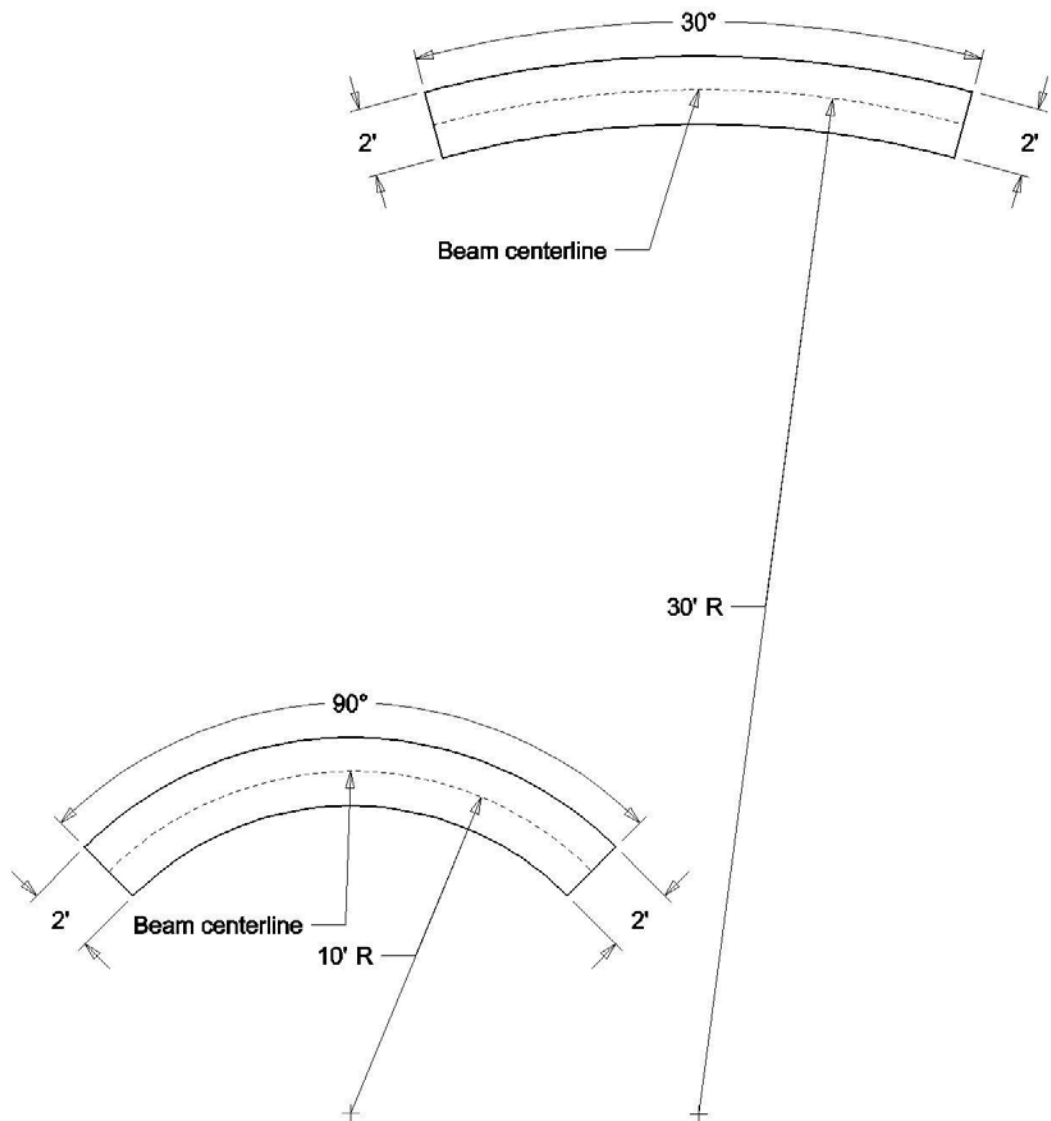


Figure 3-6 Plan view of beams

3.3.2 Materials

3.3.2.1 Concrete

Concrete mix used for both the permanent and replaceable part of the beams had nominal 28-day strength of 5,000 psi and a minimum slump of 6 in. The high slump was necessary because of the complicated forms. Slump tests were performed before each pour. Concrete strength of both permanent and replaceable part was also checked.

3.3.2.2 Concrete Debonder

To prevent bond between the replaceable and permanent parts, a concrete debonder was used. The debonder is commonly used for match casting in segmental construction. It consists of a mix of Murphy's Oil soap (generally used for cleaning wood) and talc. The mix used approximately 14 lbs of talc with one gal. of soap.

3.3.2.3 Emulsifiable Oils

The two emulsifiable oils used were TRUKUT® NC205, manufactured by CITGO Inc., and Nox-Rust® 703D, produced by Daubert VCI Inc. The oils were used as received, without adding water.

3.3.2.4 Post-Tensioning Hardware

3.3.2.4.1 Anchors

The anchors used for post-tensioning were VSL EC 12-05. However, only the anchor heads were used. The trumpet and spiral reinforcement were not needed. The anchor heads are designed for twelve 0.5-in. strands. Wedges for the anchor heads were also supplied by VSL.

3.3.2.4.2 Ducts

Three different ducts were used: a schedule 40 galvanized steel pipe, with nominal diameter of 3 in.; a corrugated galvanized steel duct supplied by VSL for their 5-12 anchors; and a High Density Polyethylene type 76 duct also supplied by VSL as part their PT-PLUS™ System.



Figure 3-7 Ducts

3.3.2.4.3 Strands

The strand used in all of the test specimens was MINILAX 0.5-in., low relaxation pre-stressing strand conforming to ASTM A416 Grade 270. All strand came from the same reel.

3.4 PROCEDURE

3.4.1 Casting of Specimens

3.4.1.1 *Permanent Part*

Because of the unusual shape of the beams, special considerations were made when building the forms for the permanent part of the beams. The forms were made out of five parts: the inner wall, the outer wall, the trough, and two end walls. Each part was built separately before they were set in place.

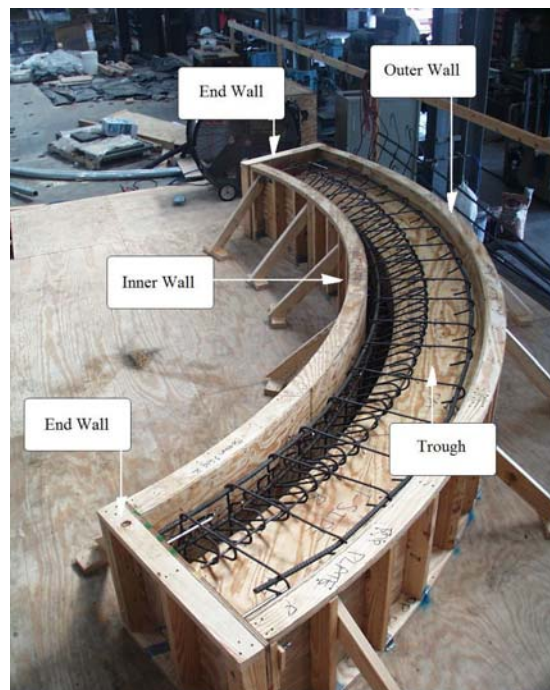


Figure 3-8 Completed forms for permanent part

Figure 3-8 shows all the form parts for the beam with a 10 ft radius of curvature. The process was identical for the beam with radius of 30 ft. However, because of the tighter curvature in the beam with a radius of 10 ft, the reinforcing bars had to be bent before the cage could be assembled. This step was not necessary in the reinforcing cage of the beam with a 30 ft radius. However, in

both cases, the reinforcing bars had to be firmly attached to the forms so they would maintain the desired shape.

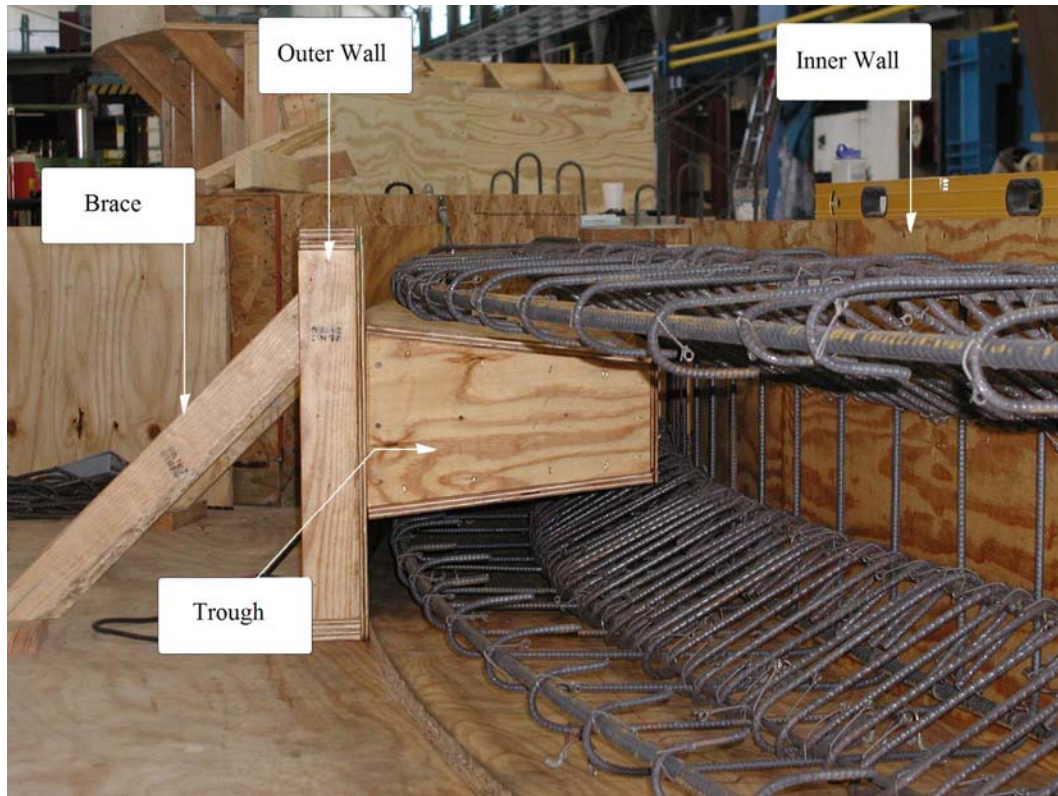


Figure 3-9 Forms for permanent part during construction

The inner wall was moved into place and attached to the floor before the rebar cage was assembled. The cage was built inside the forms in its final position before the other parts of the forms were moved into place. The trough was attached to the outer wall and afterwards moved to its position. Figure 3-9 shows a cross-sectional view of the forms and rebar cage in their final position.

After both the inner and outer walls were installed, the end walls were set in place and attached to the floor as well as to the outer and inner walls. Each end wall contained four bolts that were embedded into the concrete so that the bearing

plates could be attached to the ends of the beams. In addition, braces were added to the outer and inner walls as shown in Figure 3-8 and Figure 3-9.

After casting and removing the forms, the bottom surface inside the trough contained a large number of small depressions caused by trapped air. These depressions were filled with a mix of portland cement and water so the finished surface would be smooth.

3.4.1.2 Replaceable Part

To prevent bonding of the replaceable part and the permanent part, a concrete debonder was used. The debonder was mixed in a bucket and then applied to the inside of the permanent part before the post-tensioning duct was installed.

The procedure for the installation of the post-tensioning duct varied for each duct material. When a steel pipe was used, the pipe was supported in the middle of the beam by a wooden block and at the ends by the end walls, as shown in Figure 3-10. The end walls were attached to the permanent part by the four bolts that had been embedded into it. Caulk was used at the joints between the concrete of the permanent part and the forms to prevent concrete leaks so that the ends of the beams were smooth.

When HDPE ducts or galvanized steel ducts were used, they were held in position by pieces of styrofoam cut to the appropriate shape and inserted between the permanent part of the beam and the duct. The styrofoam supports were placed approximately every two feet as shown in Figure 3-11 and Figure 3-12. They also held the longitudinal reinforcement in place on the inner side of the replaceable part.



Figure 3-10 Installation of steel pipe



Figure 3-11 Installation of HDPE duct



Figure 3-12 Installation of galvanized steel duct



Figure 3-13 Forms for replaceable part

Once the end walls and the duct were installed, the form bottom and the side wall were set in place, attached, and braced to the floor. Figure 3-13 shows the forms ready for placing concrete on the beams with radius of curvature of 30 ft and 10 ft, on the left and the right respectively.

After the replaceable part was cast and the forms had been removed, the ducts were cut flush with the face of the concrete beam at both ends. Figure 3-14 shows the completed cross-section.



Figure 3-14 Completed cross-section

3.4.2 Preparation for Test

At the live end, a 1.5-in. thick steel bearing plate was used between the hydraulic ram and the beam. The bearing plate was intended to uniformly distribute the compressive force onto the beam. At the dead end, a similar bearing

plate was used for the same purpose. However, at the dead end, the bearing plate also had four welded pins that were used for alignment of the chair with the load cells.

Because of the uneven surface at the end of the beams, it was necessary to use a layer of hydro-stone between the face at the end of the beam and the bearing plates. The bearing plates were moved close to the end of the beam and held in place by the four bolts that came out of the concrete. Their position was adjusted with the nuts of the bolts so that a space, of approximately 1/8 in., was left between the beam and the plate. Before pouring the hydro-stone, the bottom and sides of the gap were sealed with expansive and adhesive foam (Great Stuff™) to prevent leaks. In addition, foam was used around the five holes in the bearing plates: one hole on each bolt and one hole for the post-tensioning duct. Once sealed, the hydro-stone was poured.

Because of frequent leaks of the hydro-stone, foam was used in large quantities. This left large areas of the face of the beams covered with foam instead of hydro-stone. However, the beams behaved satisfactorily during loading. No cracks were observed during post-tensioning. Figure 3-15 shows the face of the beams after the bearing plate was removed. The picture shows the areas were hydro-stone and foam covered the end of the beam.



Figure 3-15 Hydro-stone on face of beam

After the hydro-stone had hardened, the hydraulic ram and the chair with the load cells were moved to their positions at the live and dead end respectively. The steel chair shown in Figure 3-16 had two functions. First, it transferred the force from the anchor head to the load cells, and second, it created approximately the same distance from the face of the beam to the anchor head on the dead end as the hydraulic ram did on the live end.

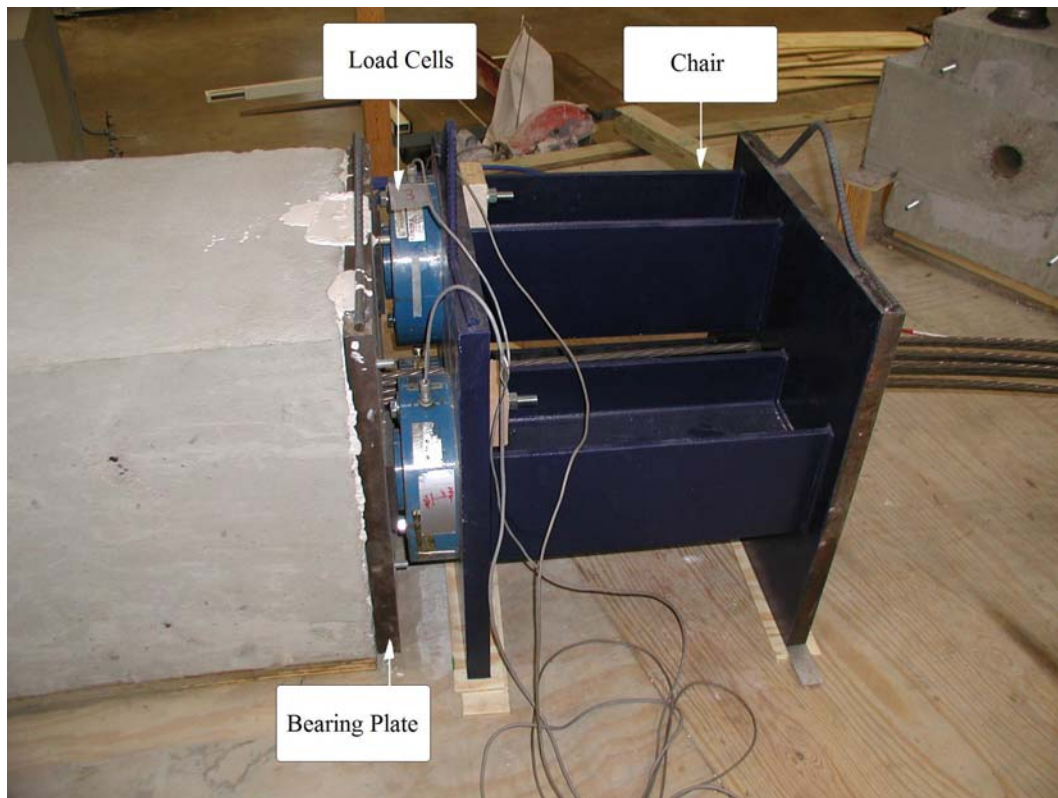


Figure 3-16 Dead end detail

Because the intention of the experiment was to recreate the conditions present in a post-tensioning duct in the middle of a member and not near the anchorages, the tendon was brought to a compact bundle by the machined holes in the bearing plates. These holes were smaller in diameter than the post-tensioning ducts. In order to reduce the bending of the strands where they were forced into a compact bundle, a distance of about 28 in. was left between the bearing plate and the anchor heads. At the live end, this distance was provided by the hydraulic ram; at the dead end it was provided by the steel chair.

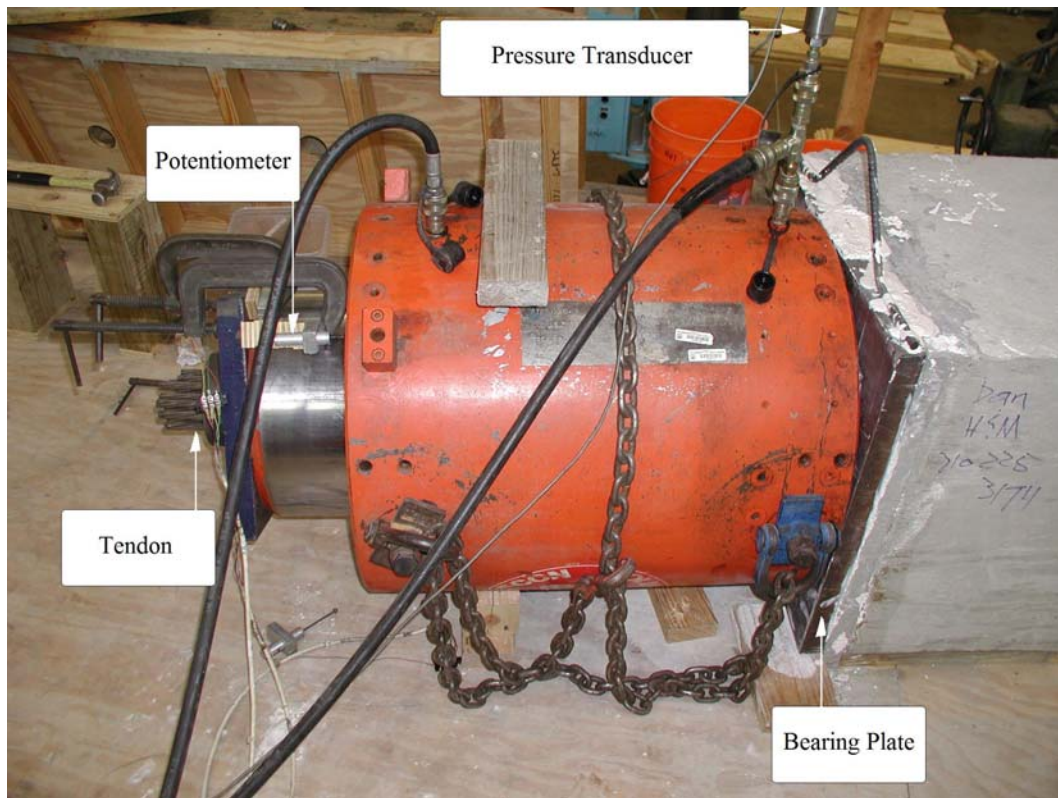


Figure 3-17 Live end detail

Twelve, 25-ft long strands were cut and bundled together into a tendon with duct tape at one end. On top of the duct tape, a piece of cloth was wrapped around the tendon for easier feeding. The tendon was fed from the dead end. Once the tendon had been placed, the hydraulic ram was extended approximately 6 in. to allow enough space between the anchor head and the hydraulic ram for cutting the tendon with a grinder after the test had been completed. At both the live and dead end, the wedges were hammered in for better seating. Afterwards the pressure transducer and the potentiometer were installed as shown in Figure 3-17.

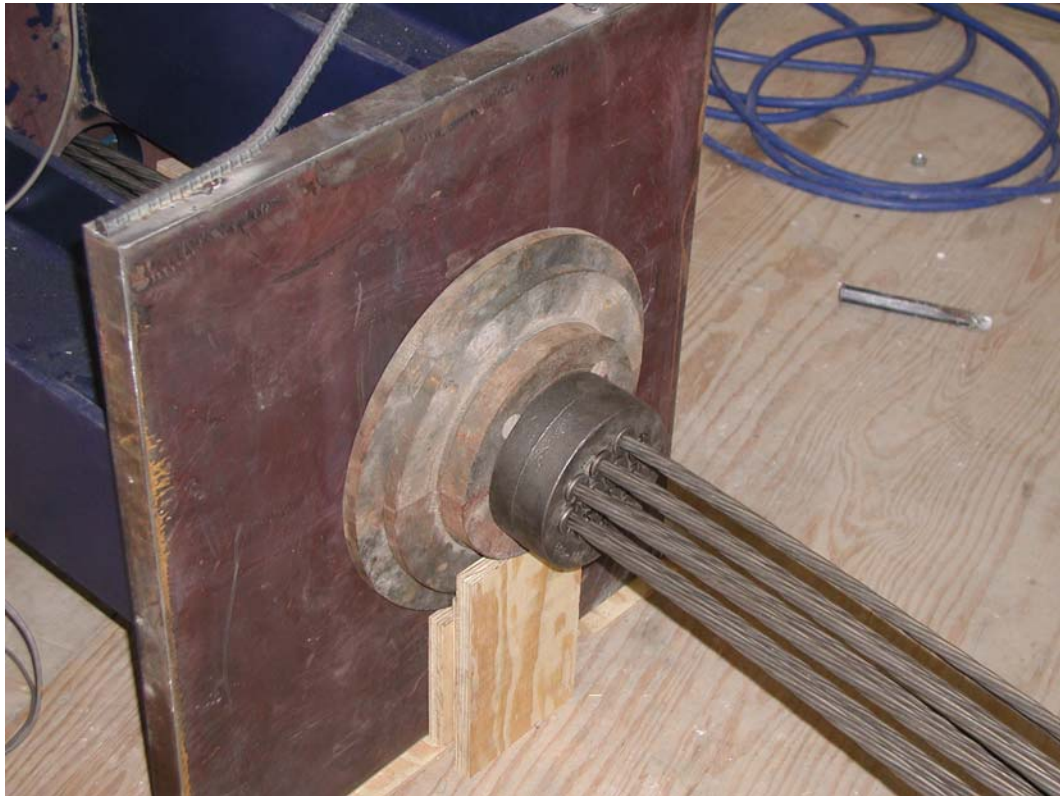


Figure 3-18 Split rings on dead end

At the dead end, three split rings were used as spacers between the anchor head and the steel chair. Two of the split rings were $\frac{3}{4}$ in. thick and one was 1 in. thick. One split ring was removed every time the tendon was stressed, starting with the $\frac{3}{4}$ in. thick ones that were positioned farthest away from the anchor head. In this way, the tendon moved relative to the post-tensioning duct every time it was stressed, so that the contact surfaces were different for every loading and the friction losses for every loading would be as close as possible to the first loading. The installed split rings are shown in Figure 3-18. The split rings also gave more space between the anchor head and the beam for cutting the tendon after the test had been completed.

The tendon was oiled using a garden sprayer, as seen in Figure 3-19. Oil was sprayed abundantly, to ensure good lubrication. However, because the tendon was sprayed from the top, the bottom surfaces of the strands were not always initially covered with oil. However, the oils did flow through the interstices of the strands; all of the strand's surfaces were covered with oils when the strands were removed from the duct, after completion of the test.



Figure 3-19 Oiling of tendon

3.4.3 Test Sequence

There were a total of 6 rounds of tests: two oils tested on three different duct materials. Each round of tests consisted of 3 dry tests, 2 oiled and tested immediately, and 2 oiled and tested a day after application of the oil; all of these

tests were performed on each beam. The next round of tests was done using the same duct material, but different oil. Consequently, for every duct material there were a total of 6 dry tests on each beam.

In each round, a total of seven tests (loadings) were done on every beam before the replaceable part was changed. On every loading, readings were taken approximately every 10 kips. Two tendons were used in each beam. The first tendon was not oiled and was used on the first three loadings. After the first loading, the first $\frac{3}{4}$ in. split ring was removed and the hydraulic ram extended to close the gap. The same was done after the second test. After the third test, the only remaining split ring (1 in. ring) was removed and the hydraulic ram retracted completely; this allowed access to the tendon for cutting it with a grinder. Once the tendon was cut, it was removed from the beam. Afterwards, the second tendon was oiled and fed into the beam. This tendon was stressed four times. The first two were done immediately after installation of the tendon, while the other two were done the next day. After the first and second loadings, the two $\frac{3}{4}$ in. split rings were removed, and after the third loading, the 1 in. split ring was removed.

The seven tests were first performed on the beam with a radius of curvature of 30 ft, and then on the one with a radius of 10 ft. Having completed the tests, both replaceable parts were removed, and the beams were ready for the next round of tests.

3.4.4 Removal of Replaceable Part

The replaceable part was removed after the seven tests were completed on the beam. The tendon, hydraulic ram, chair and load cells, and both bearing plates were detached in preparation for removal. The setup for removal is shown in Figure 3-20 and Figure 3-21. Two small hydraulic rams were inserted between the permanent part and a W8x40. The W8x40 pulled on a chain attached to a concrete

anchor embedded in the replaceable part. Each beam had two anchors; however, they were not pulled at the same time.

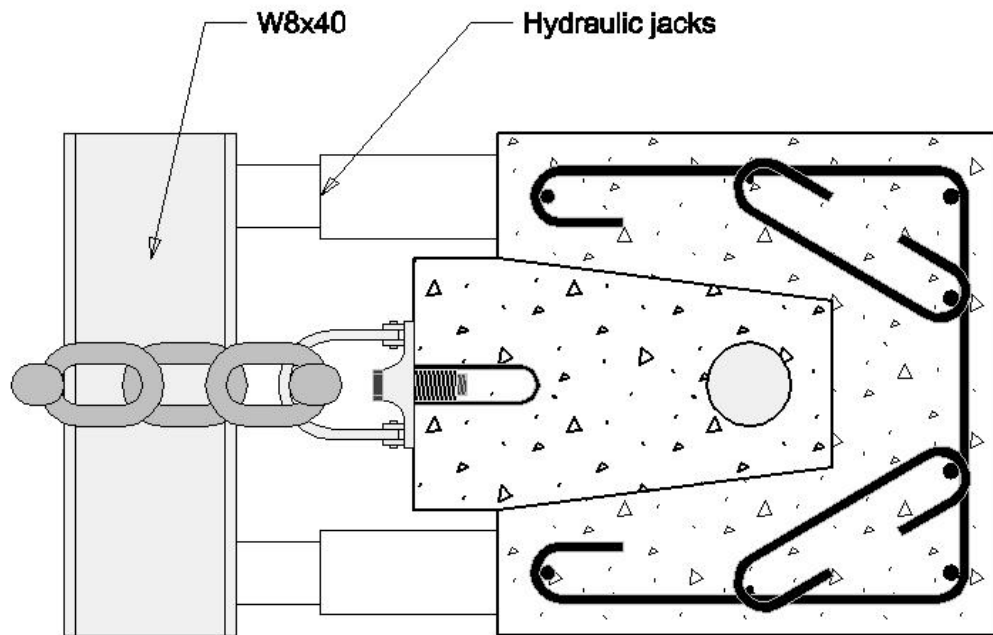


Figure 3-20 Separation of permanent and replaceable part

Once the replaceable part had separated about 1 in. from the permanent part, the W8x40 was removed and the two anchors were attached with chains to an overhead crane. The crane lifted the replaceable part while it was pushed out of the permanent part with a crowbar. The inside of the permanent part was then cleaned of debonder residue. At this point the process started again from the beginning: applying the debonder to the permanent part and installing the post-tensioning duct inside the permanent part. The separation process worked very well.



Figure 3-21 Removing replaceable part

3.4.5 Determination of Hardware Losses

In order to correctly estimate the friction losses in each specimen, it is necessary to also determine the losses at the anchorages, caused by the stressing hardware. These losses may be caused by the hydraulic ram or by friction between the bearing plates and the tendon. In practice these losses are usually very small compared to the friction losses. However, because the specimens tested here were shorter than those used in practice, these small losses may be significant.

The setup for determining the hardware losses consists of setting up all of the stressing hardware and instrumentation in the same way as if a normal test

was to be performed, but omitting the concrete specimen itself. This setup is shown in Figure 3-22.

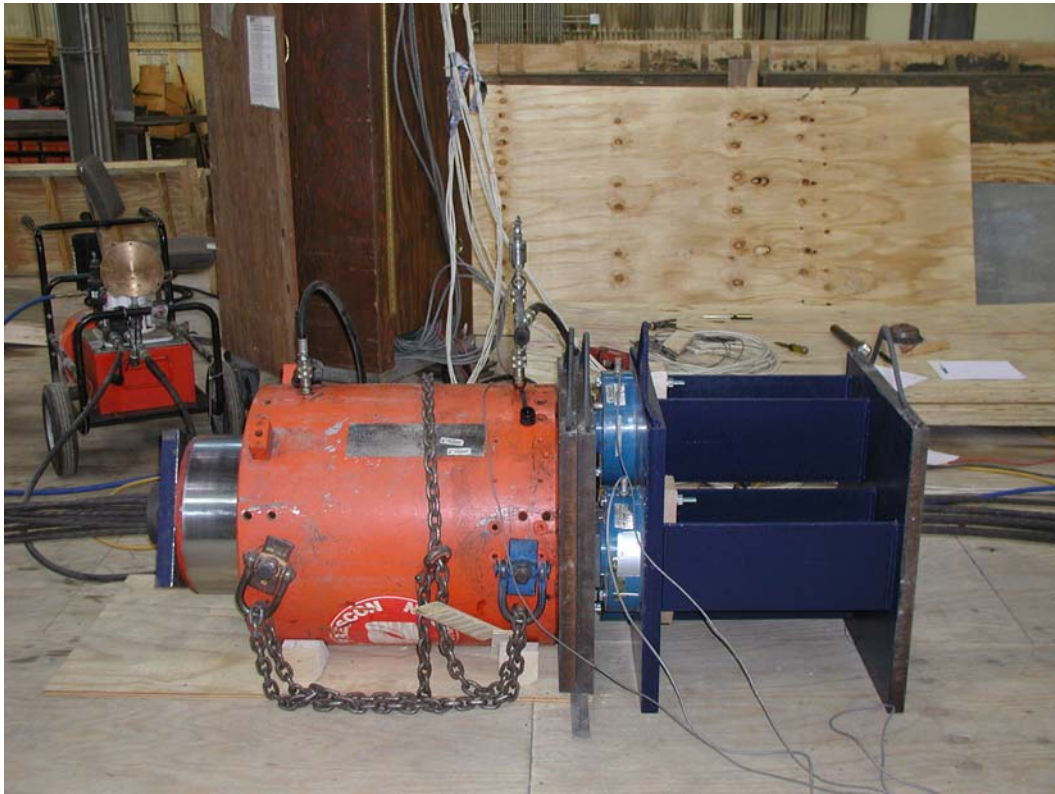


Figure 3-22 Determination of hardware losses

A total of eleven of these special tests were performed: three dry, two oiled and stressed immediately, and two oiled and stressed a day after. These last four tests were repeated for the two different oils.

CHAPTER 4

Test Results

This chapter presents the results from all tests. It is divided into two sections. One section contains the results of the friction tests. The other one shows the condition of the post-tensioning ducts after they were removed from the beams. This last section shows the damage done to the ducts by the strands as they were stressed.

4.1 FRICTION TEST RESULTS

This section is divided into four sub-sections. The first three contain the results of the friction tests for each duct material, and the last one gives the results of the hardware losses tests. Each of the first three sub-sections contains the results for both the beams with a radius of curvature of 30 ft and total angle change of 30 degrees and the beams with radius of 10 ft and total angle change of 90 degrees.

Table 4-1 Specimen name scheme

	Value	Parameter
Oil Used	0	No Oil
	1	TRUKUT® NC205
	2	Nox-Rust® 703D
Duct Material	SP	Steel Pipe
	HD	HDPE duct
	GD	Galvanized Steel Duct
Curvature	30°	Radius of curvature of 30 ft and total angle change of 30 degrees
	90°	Radius of curvature of 10 ft and total angle change of 90 degrees

Each specimen is designated by a name consisting of three parts. The first part indicates the oil used, the second indicates the duct material and the third the curvature of the specimen. Table 4-1 shows the scheme used for the specimen names.

For example, specimen 1-SP-90° is a beam with a steel pipe, radius of curvature of 10 ft, total angle change of 90 degrees, and oiled with TRUKUT® NC205.

It is important to note that seven tests were performed on each specimen, the first three of which were never lubricated (tests *Dry 1*, *Dry 2*, and *Dry 3*), the next two were lubricated with an emulsifiable oil and tested immediately (tests *Freshly Oiled 1* and *Freshly Oiled 2*), and the last two, oiled but tested after a day (tests *One Day After Oiling 1* and *One Day After Oiling 2*). For the first three tests the oil used in the specimen is irrelevant, since it was never oiled.

The names of all of the specimens start with either a 1 or a 2, because they were all eventually oiled. There is only one exception to this rule. There was one specimen which was never oiled. It is designated by the name 0-SP-90°. This specimen had a steel pipe, a radius of curvature of 10 ft, and a total angle change of 90 degrees. As with all other specimens, seven tests were performed on this specimen, and the test procedure was exactly the same as in any other specimen, the only difference was that this one was never oiled. Therefore, tests *Dry 4* and *Dry 5* of this specimen correspond to tests *Freshly Oiled 1* and *Freshly Oiled 2* of any other specimen, and tests *Dry 6* and *Dry 7* correspond to tests *One Day After Oiling 1* and *One Day After Oiling 2*.

The results of the seven tests are shown on a single graph for each specimen. Each graph shows the percent loss plotted against live end load. The percent loss is calculated as the difference in load between the live and dead end

divided by the live end load. The results shown are total losses and include hardware losses. In order to determine friction losses, hardware losses must be subtracted from the total losses. This will be explained further in Chapter 5.

Because in practice tendons are usually stressed to loads in the range of 70% to 80% of their capacity, only the data points in that range are of interest. Therefore, all values below 70% of the capacity are not of interest and are shaded in the plots. The capacity of a 0.5-in., twelve-strand tendon is 496 kips; 80% of the capacity is 397 kips, and 70% of the capacity is 347 kips.

4.1.1 Steel Pipe

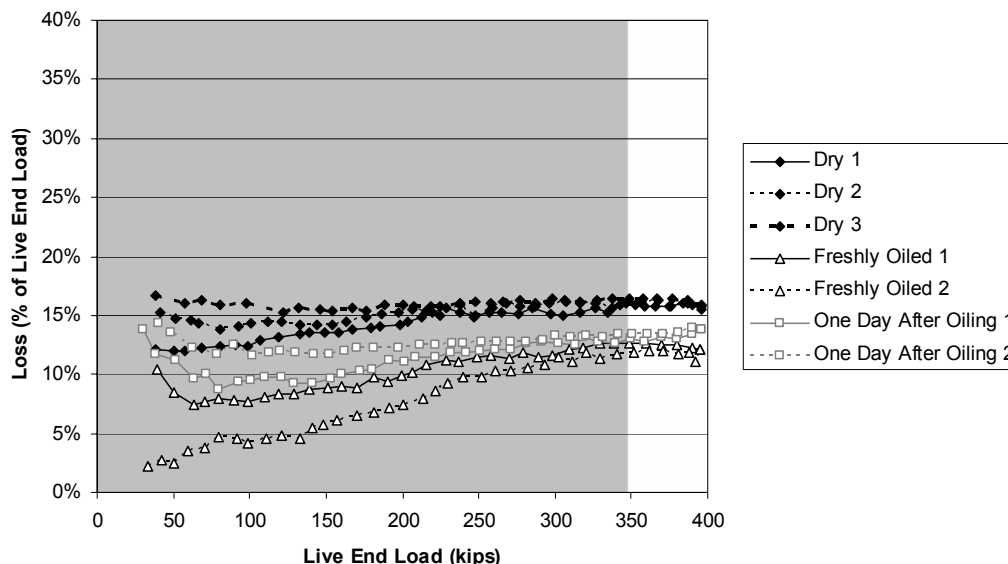


Figure 4-1 Specimen 1-SP-30°

Figure 4-1 show the results of the specimens with a radius of curvature of 30 ft and oil NC205. The plot shows consistent results within each type of test: *Dry*, *Freshly Oiled*, and *One Day After Oiling*. Although, initially there is significant scatter in all curves, as they approach the region of interest (high loads) the curves for each type of test tend to group together. The average loss for

the *Dry* tests is about 16%, while in the *Freshly Oiled* it is around 12%, and 13% in the *One Day After Oiling*.

The next specimen, shown in Figure 4-2, has similar behavior to the previous one; the only difference between the two was the oil used (oil 703D). There is very little scatter in the region of interest, especially for the *Freshly Oiled* and *One Day After Oiling* tests. However, apparently there is less loss in this specimen than in the previous one. The average loss in the *Dry* tests is 13%, while in the *Freshly Oiled* and *One Day After Oiling* are 8% and 9.5% respectively.

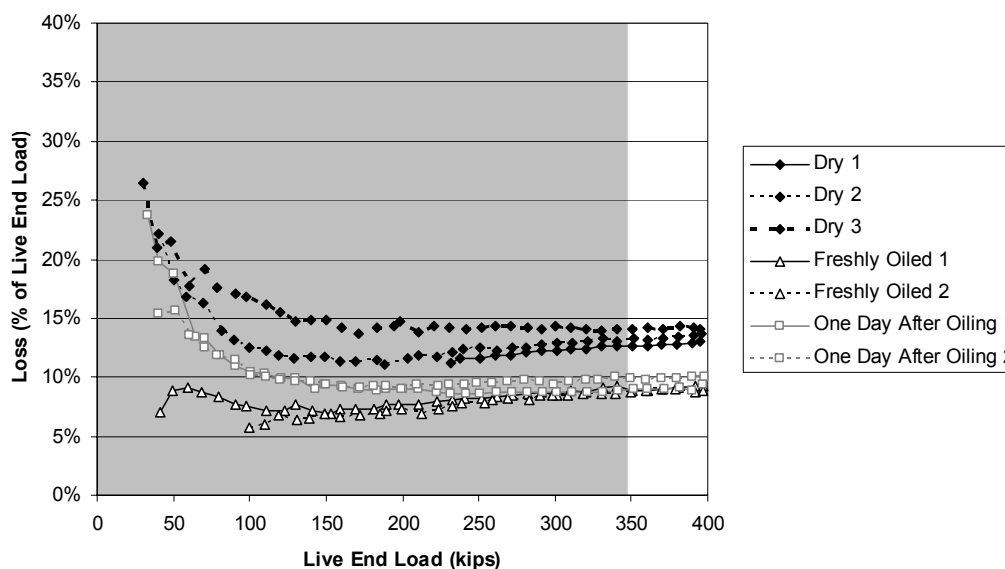


Figure 4-2 Specimen 2-SP-30°

The next three specimens have a radius of curvature of 10 ft and total angle change of 90 degrees. Because of the sharper curvature, higher losses are expected. The first one, shown in Figure 4-3, was never oiled. However, it is useful for comparing with the next two. The behavior of this specimen shows considerably more scatter than any of the previous ones. Load loss seems to increase from test to test, up to the fourth one, where the friction drops again, but

keeps increasing in the consecutive ones. At the fourth test, the strand was changed for consistency with all other specimens. The average load loss of the seven dry tests was 32% with a range from 29% to 35%. However, like most other test, in the region of main interest the scatter decreases and most curves tend to group together.

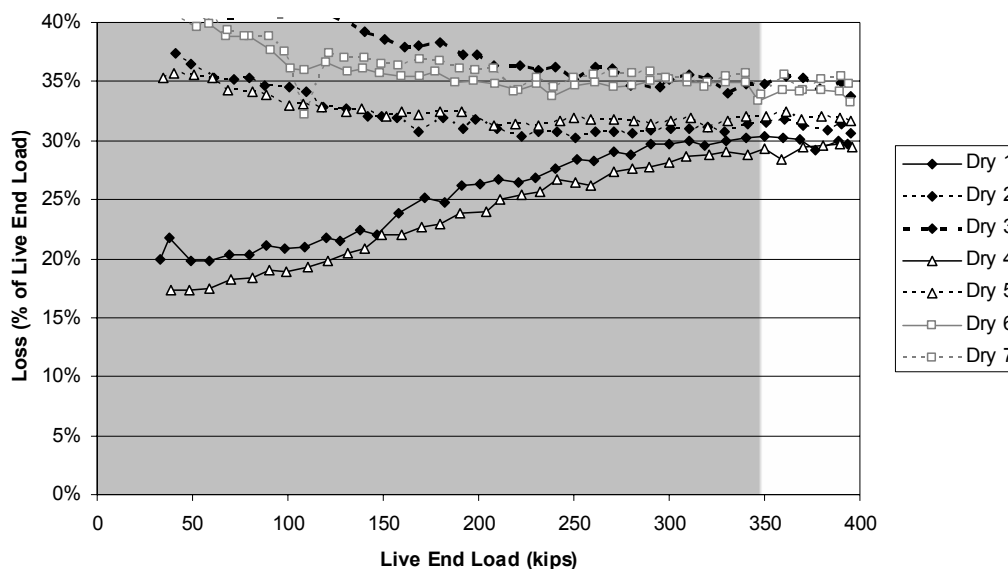


Figure 4-3 Specimen 0-SP-90°

Specimen 1-SP-90°, shown in Figure 4-4, has about the same load loss in the *Dry* tests as the previous specimen, between 29% and 36% with an average of 33%. On the other hand, the loss for the *Freshly Oiled* tests (with averages of 27% and 30% for first and second test respectively) was lower than for the *One Day After Oiling* (approximately 34% for both tests).

Similarly, specimen 2-SP-90°, shown in Figure 4-5, has average losses in the *Dry* tests between 28% and 32% and less average loss in the *Freshly Oiled* tests, 21% and 25% on the first and second one respectively, compared to the *One Day After Oiling* tests, 30% and 33% for the first and second tests respectively.

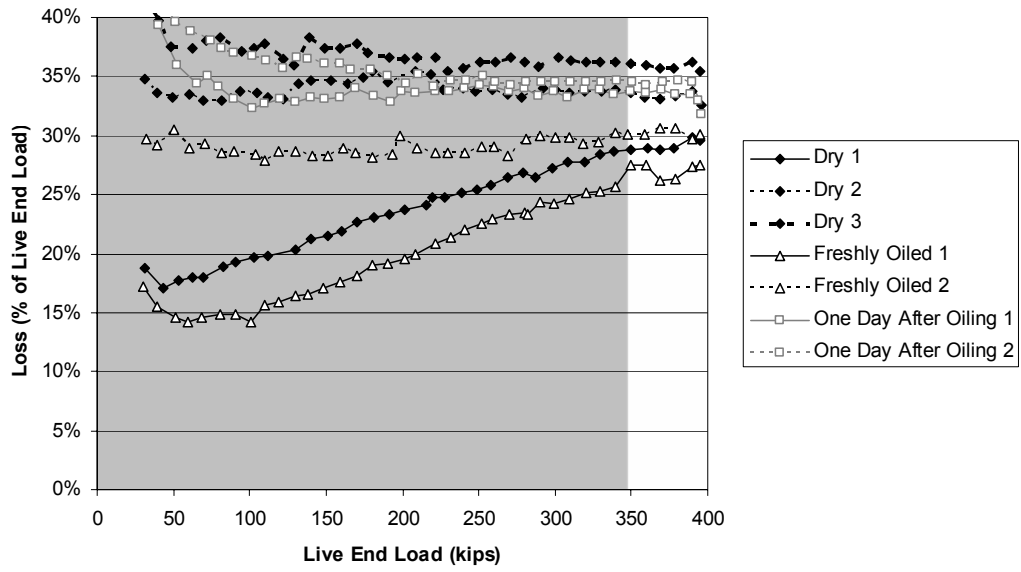


Figure 4-4 Specimen 1-SP-90°

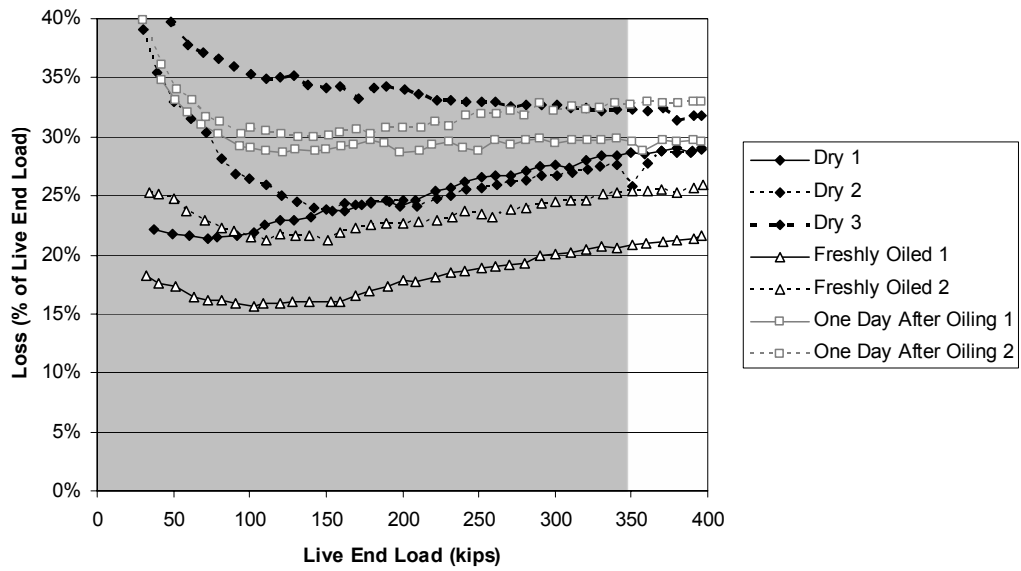


Figure 4-5 Specimen 2-SP-90°

4.1.2 HDPE Duct

Results from the next four specimens with plastic ducts showed considerable less load loss when compared with the steel pipe specimens. Therefore, it was necessary to change the scale in the graphs in order to evaluate the response.

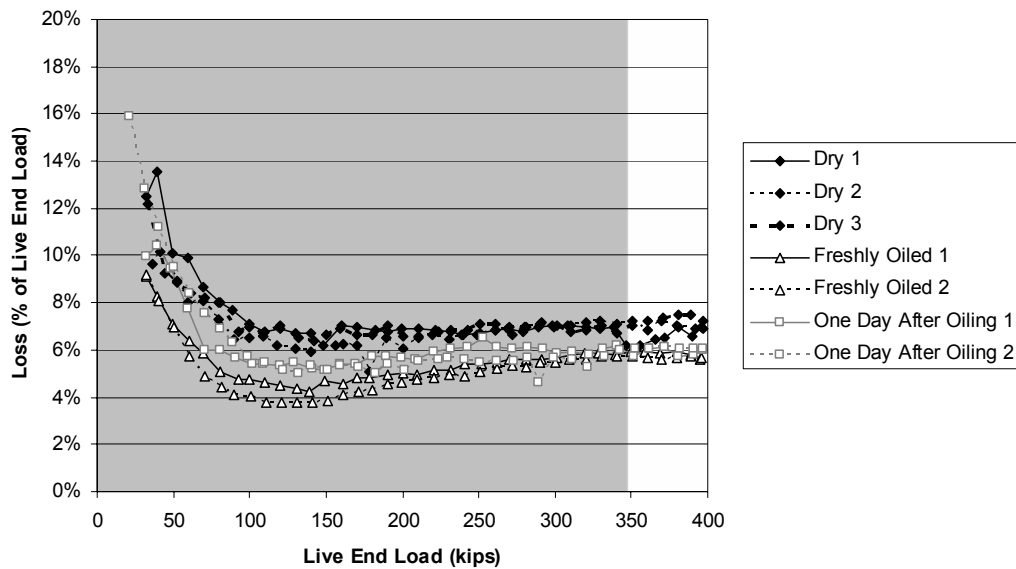


Figure 4-6 Specimen 1-HD-30°

The results from specimens 1-HD-30° and 2-HD-30°, shown in Figure 4-6 and Figure 4-7 respectively show little scatter. Specimen 1-HD-30° has load losses in the *Dry* tests around 7%, while in the *Freshly Oiled* and *One Day After Oiling* tests losses are around 6%; while specimen 2-HD-30° has load losses slightly above 6% for both the *Dry* and *One Day After Oiling* tests, and slightly below 6% for the *Freshly Oiled* tests.

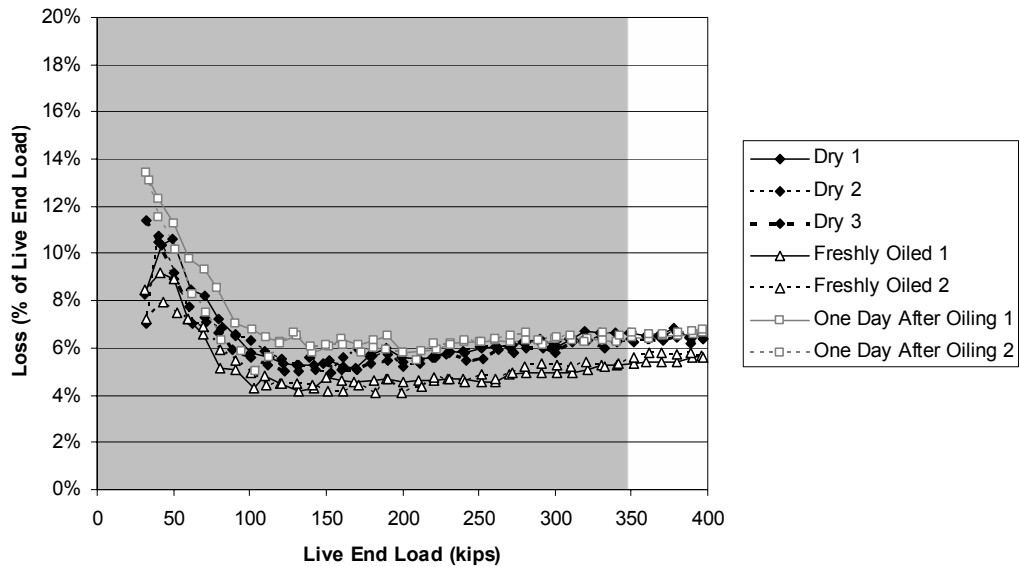


Figure 4-7 Specimen 2-HD-30°

In specimens 1-HD-30° and 1-HD-90°, as the strands were being removed, they showed sharp bends in the location where they passed through the bearing plates. Figure 4-8 shows the sharp bend in the strand after it was removed. This sharp bend was probably caused by misalignment of the bearing plate and the duct. However, its effect on the friction loss seems insignificant, since the load loss on the *Dry* tests of both specimen 1-HD-30° and 2-HD-30° is the same, approximately 7%. The same is true for specimens 1-HD-90° and 2-HD-90°. In both specimens the load loss on the *Dry* tests is approximately 18%.

Unfortunately, this sharp bend caused several wires to break during testing of specimen 1-HD-30° and 1-HD-90°. In the last test (*One Day After Oiling 2*) of specimen 1-HD-90°, shown in Figure 4-9, it was impossible to test beyond 320 kips because wires kept breaking as attempts were made to increase the load. However, from the curves it seems that similar losses in load were occurring in both tests (*One Day After Oiling 1* and 2).



Figure 4-8 Sharp bend on strand

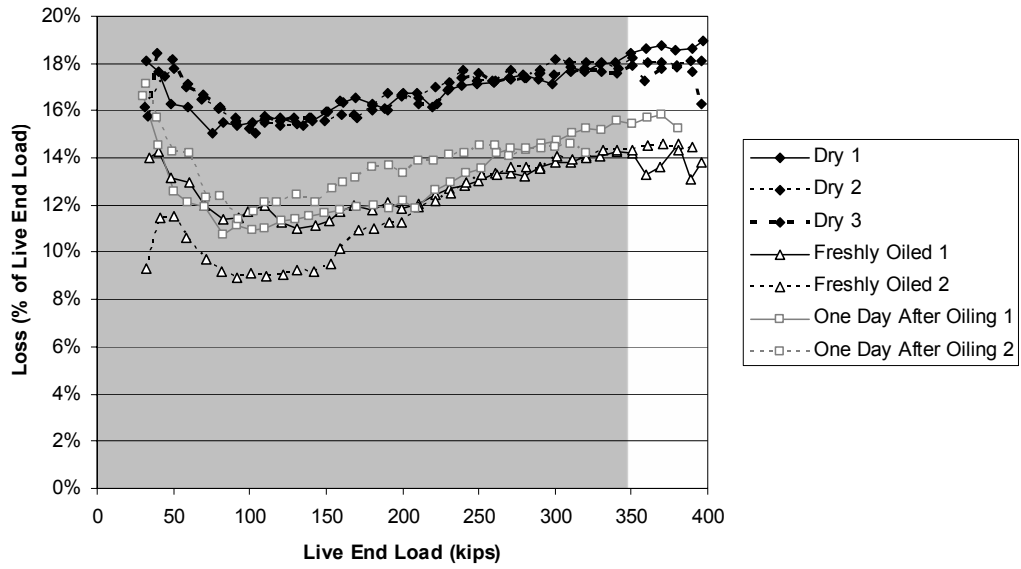


Figure 4-9 Specimen 1-HD-90°

Results from test *Dry 3* in specimen 2-HD-90°, shown in Figure 4-10, have an unexpected increase in the load loss when the live end load is about 170 kips. The data points are out of the range of the plot. Careful review of the data showed the load dropped significantly on one load cell, while the load on the other two increased as expected. This is obviously an error, and was probably caused by the electronic equipment. These data will not be used. The rest of the data indicated that loss on the *Dry* tests averaged 18%, and 15% for both the *Freshly Oiled* and *One Day After Oiling* tests.

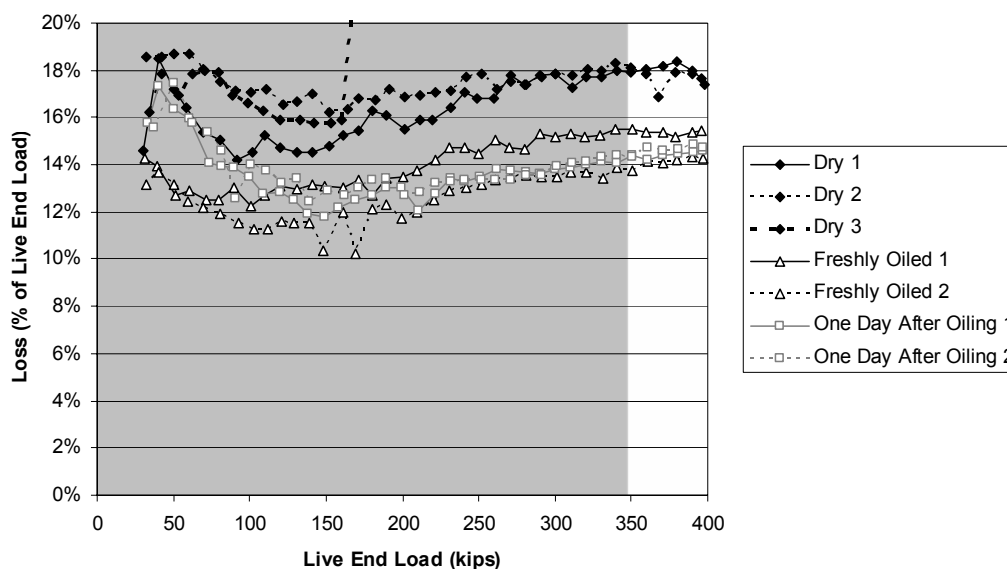


Figure 4-10 Specimen 2-HD-90°

4.1.3 Galvanized Steel Duct

All specimens using a galvanized steel duct had higher losses than those using HDPE ducts. Specimens 1-GD-90° and 2-GD-90° showed losses in the same range as those using steel pipes. Therefore, in all figures in this section the scale was changed to what was used in the steel pipe specimens.

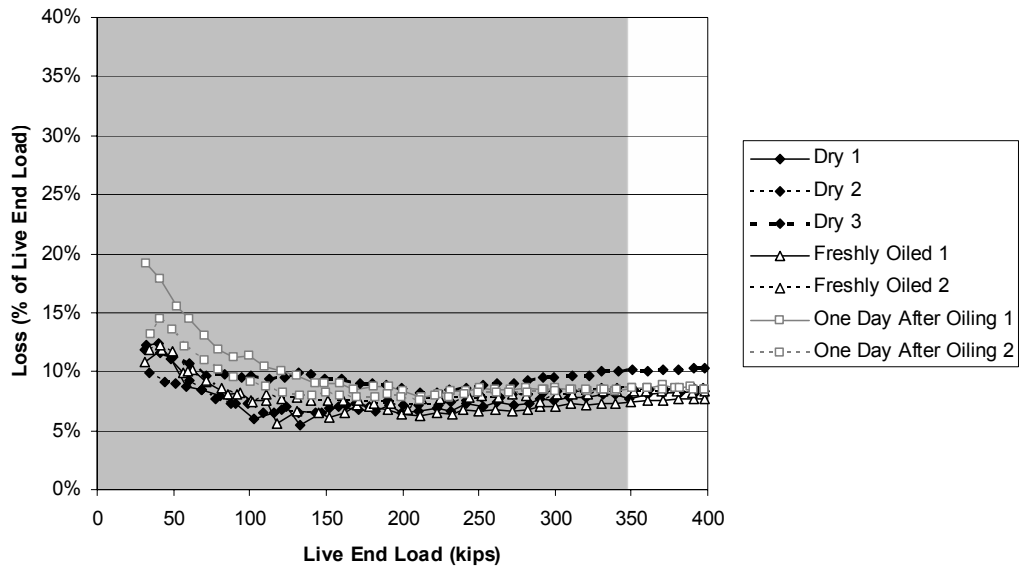


Figure 4-11 Specimen 1-GD-30°

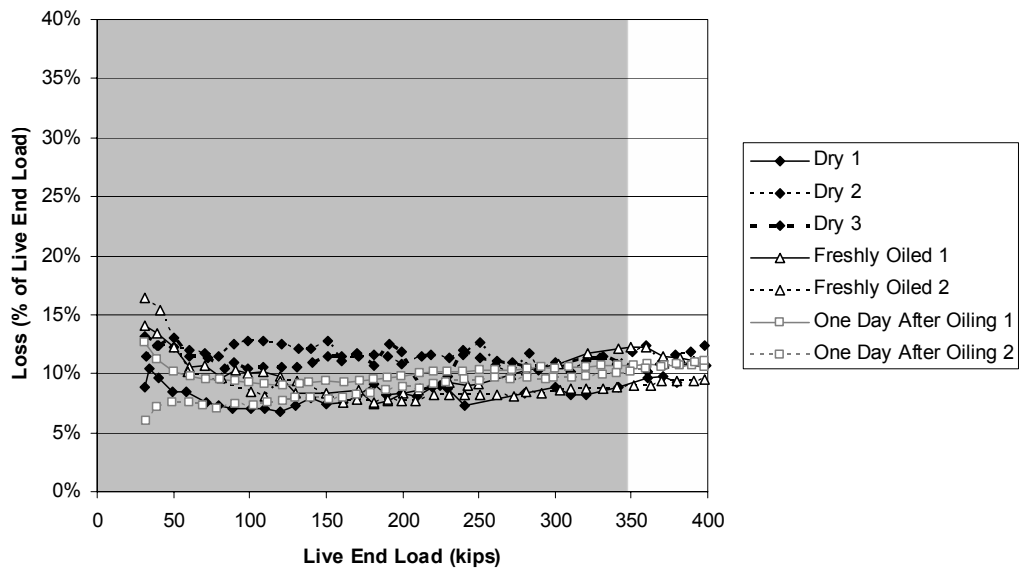


Figure 4-12 Specimen 2-GD-30°

Figure 4-11 shows the results from specimen 1-GD-30°. The losses for all tests are very close, approximately 8%, with the exception of the third Dry test,

where the loss is about 10%. Specimen 2-GD-30°, shown in Figure 4-12, has similar results with average losses of 11% in each type of test.

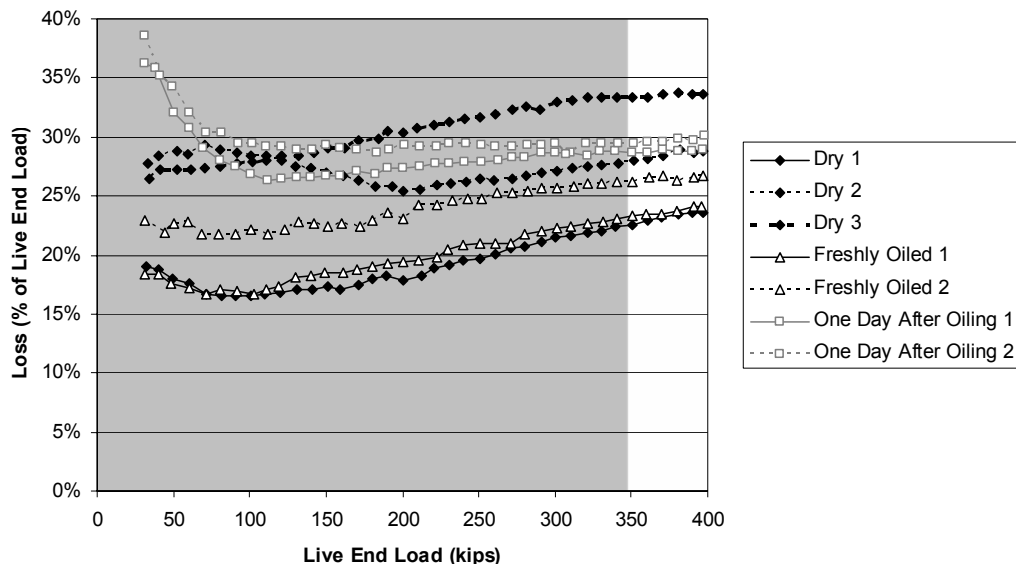


Figure 4-13 Specimen 1-GD-90°

Both specimens 1-GD-90° and 2-GD-90°, shown in Figure 4-13 and Figure 4-14, respectively, have significant scatter. But similar to specimens 1-GD-30° and 2-GD-30°, the losses in the *Dry* tests are in the same range as those from the *Freshly Oiled* and *One Day After Oiling* tests. Losses in specimen 1-GD-90° averaged 28% in the *Dry* tests, 25% in the *Freshly Oiled* and 29% in the *One Day After Oiling* tests. Losses in specimen 2-GD-90° averaged 28% in the *Dry* tests, 27% in the *Freshly Oiled* and 29% in the *One Day After Oiling* tests.

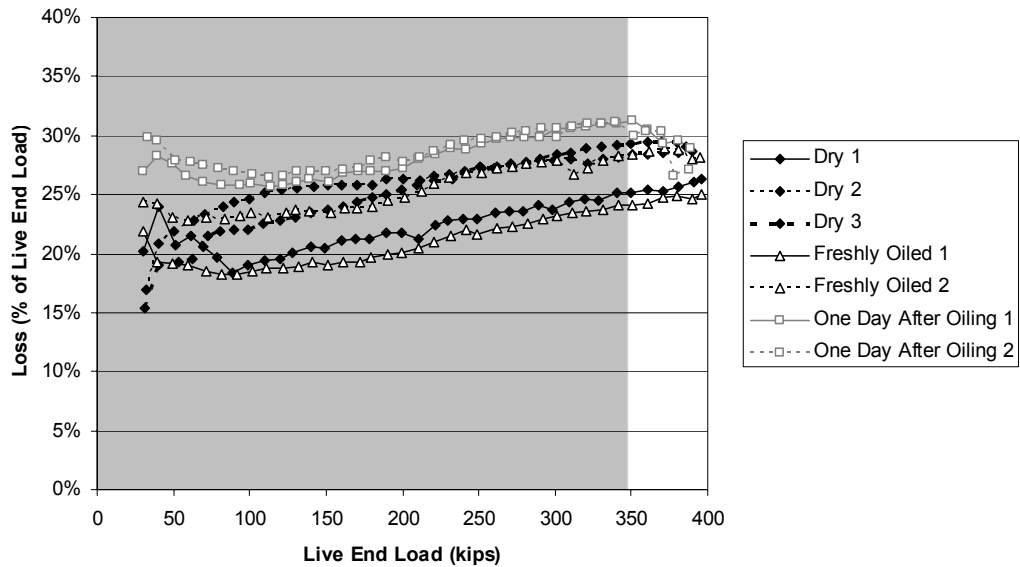


Figure 4-14 Specimen 2-GD-90°

4.1.4 Hardware Losses

Hardware losses were determined for the three tendon conditions used in the specimens: dry, oiled and stressed immediately, and oiled and stressed a day after. A total of nine tests were performed: three *Dry*, two *Freshly Oiled*, and two *One Day After Oiling*; repeating the last four tests for the two different oils. The results are shown in Figure 4-15 and Figure 4-16. In both figures the results for the *Dry* tests are the same. They were repeated to compare the dry results with the oiled results.

Calibration tests were performed at three different points in time. The first two dry tests were performed before any tests were performed on any specimen. All of the tests using oil NC205 were performed after testing specimens 1-SP-30° and 1-SP-90°. The third dry test and all tests using oil 703D were performed after all other specimens had been tests with the exception of specimens 2-GD-30° and 2-GD-90°. Both figures show that the losses in tests *Dry 1* and *Dry 2* are

significantly higher than in test *Dry 3*, about 5 times higher. This difference was probably caused by the wearing of the center-hole in the bearing plates as they were used. Initially the surface of the center-hole was machined and very smooth, but after a few tests, grooves could be seen in the surface where the strands were bearing on the plate.

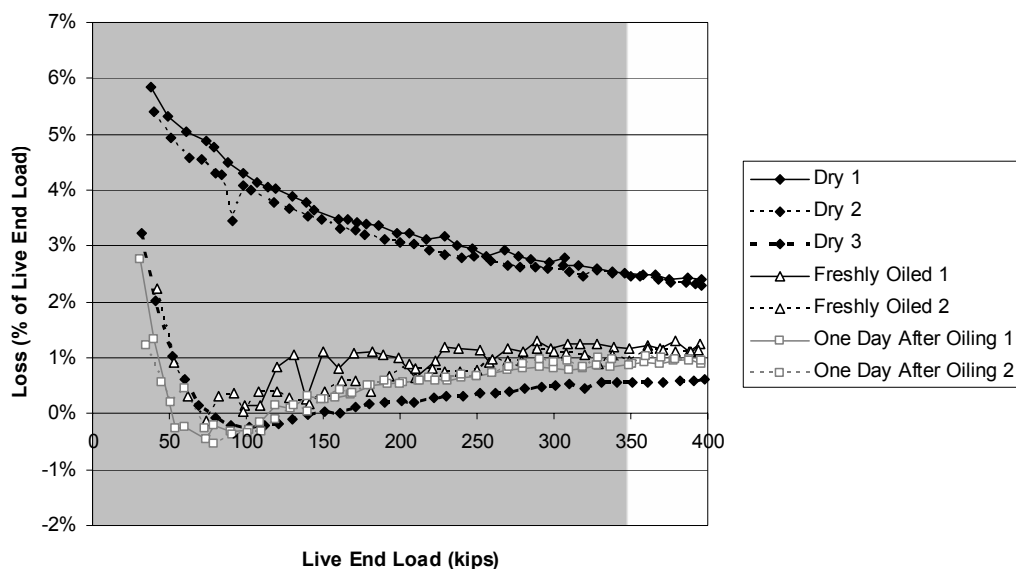


Figure 4-15 Hardware losses - oil NC205

All tests performed at the same time, independent of whether they were oiled or not, show the same loss. The first two *Dry* tests have the same value of about 2.4% in the range of interest. All of the tests using oil NC205 have a loss of 1%, while the third *Dry* test and all tests using oil 703D have a loss of 0.5%. Therefore, it appears that the hardware losses are a function of the condition of the bearing plates and not whether the tendon was lubricated.

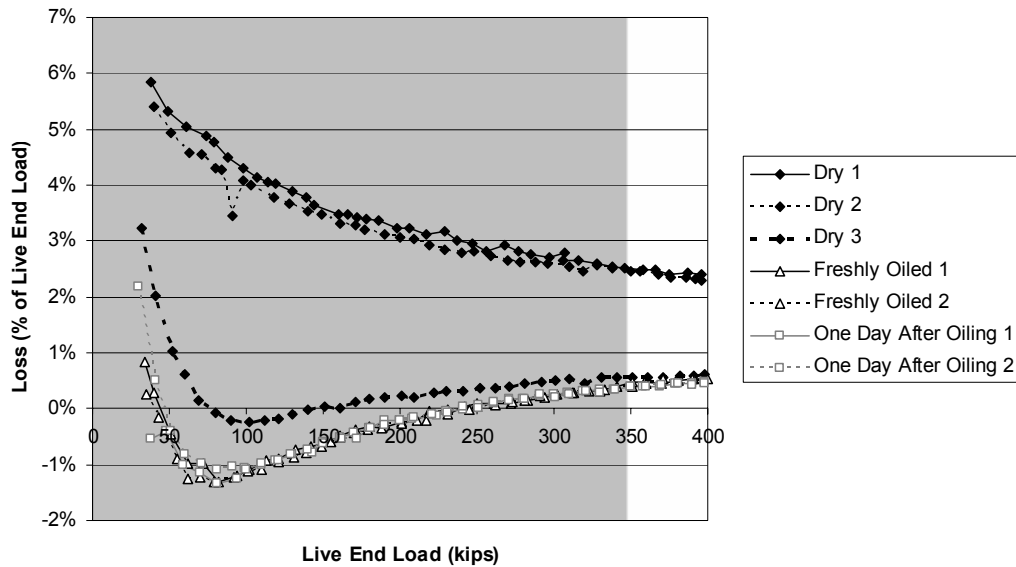


Figure 4-16 Hardware losses - oil 703D

At lower loads, although not of interest, it is seen that there are negative losses. This means that the load measured at the dead end by the load cells was higher than the load measured by the pressure transducer at the live end. This is caused by experimental errors. The load at the dead end can not be higher than at the live end. The difference is due to measurements error in both the pressure transducer and the load cells. This is especially true at low loads where the instruments are known to be inaccurate. However, this is irrelevant, because no matter what causes the difference, as long as the value of this difference is known and the data from the specimens' tests corrected appropriately, the difference in load between the live end and the dead end in the specimens may be accurately measured. So even if what is called hardware losses is due to that and other causes, the effect is the same. In this light, the hardware losses tests are more appropriately calibration tests.

Given this information, hardware losses for all specimens will be taken as 0.5% regardless of lubrication. The only exceptions are specimens 1-SP-30° and 1-SP-90°, where hardware losses will be taken as 1%.

4.2 DAMAGE TO THE POST-TENSIONING DUCTS

Removing the post-tensioning ducts from the replaceable part of the beam without damaging them required considerable care. The severe damage seen in the ducts was caused by the removal process and not by stressing of the tendon. The pictures also show oil residue remaining in the ducts. The damage caused by bearing of the strands to the ducts is seen as scrapings on the surface of the ducts.



Figure 4-17 Damage in specimen 1-HD-30°

Specimens 1-HD-30° and 2-HD-30° shown in Figure 4-17 and Figure 4-18, respectively, have visible but limited damage to the ducts. While specimens 1-HD-90° and 2-HD-90°, shown in Figure 4-19 and Figure 4-20, respectively, have more damage. This is expected since tighter curvatures puts higher normal forces to the ducts. In all four specimens the damage was not unreasonable. The integrity of the ducts does not seem to have been compromised.

Specimens 1-HD-90° and 2-HD-90° show a mark outside of the bundle. It is not known for certain what caused this damage. The possibility of a broken wire hitting the wall of the duct has been ruled out because no wires broke in specimen 2-HD-90°. The location of the damage indicates that feeding of the tendon might have been caused it.



Figure 4-18 Damage in specimen 2-HD-30°



Figure 4-19 Damage in specimen 1-HD-90°



Figure 4-20 Damage in specimen 2-HD-90°



Figure 4-21 Damage in specimen 1-GD-30°



Figure 4-22 Damage in specimen 1-GD-90°



Figure 4-23 Damage in specimen 2-GD-30°



Figure 4-24 Damage in specimen 2-GD-90°

The same trend appears on the specimens with galvanized steel ducts. Specimens 1-GD-30°, shown in Figure 4-21, has less damage than specimen 1-GD-90°, shown in Figure 4-22. The same is true for specimen 2-GD-30°, shown in Figure 4-23, and specimen 2-GD-90°, shown in Figure 4-24. The mark outside of the bundle that appeared in specimens 1-HD-90° and 2-HD-90° does not appear in either specimens 1-GD-90° or 2-GD-90°.

CHAPTER 5

Evaluations of Test Results

5.1 INTRODUCTION

The results presented in Chapter 4 were the percent load loss from the live end to the dead end. This percent load loss is due three components: curvature friction loss, wobble friction loss, and losses at the anchorages. The only component of interest in this study is curvature friction loss.

Losses at the anchorages were measured from the hardware loss tests, and can be properly accounted for. The wobble friction losses are assumed to be negligible. The wobble friction losses are due to unintended angle changes. Because the specimens were carefully constructed in a laboratory, wobble losses are expected to be very small. In addition, the specimens had large angle changes, 30 and 90 degrees, and relatively short length, 15.71 ft. This makes the curvature friction losses considerably larger than the wobble friction losses. For example, using the wobble and friction coefficient recommended by AASHTO of 0.0002 1/ft and 0.15, respectively, the expected losses for a specimen with galvanized steel ducts and a total angle change of 30 degrees are as follow:

$$\begin{aligned}P_B &= P_A e^{-(\mu\alpha + KL)} \\P_B &= P_A \left(e^{-\mu\alpha} \right) \left(e^{-KL} \right) \\P_B &= P_A \left(e^{-0.15 \times 30 \frac{\pi}{180}} \right) \left(e^{-0.0002 \times 15.71} \right) \\P_B &= P_A (0.924)(0.996)\end{aligned}$$

This example shows that the reduction in force along the tendon due to curvature friction is about 7.6%, while that due to wobble friction is about 0.3%. The wobble losses are an order of magnitude smaller than the curvature friction

losses. This example was carried out using the specimen with the lowest expected curvature friction loss. In a specimen with a higher curvature friction coefficient and more angle change, the curvature friction losses will be greater. In addition the actual wobble friction coefficient in these experiments is certainly smaller than the one used in the example. Therefore it is the author's opinion that assuming no wobble loss for these tests is well justified.

Table 5-1 shows the percent load loss of all tests averaged over the load range of interest. This range is from 70% to 80% of the tensile capacity of the tendon. Correcting the data by subtracting the hardware losses yields the losses due only to curvature friction, shown in Table 5-2.

Table 5-1 Average Percent Load Loss

Specimen	Test						
	Dry 1	Dry 2	Dry 3	Freshly Oiled 1	Freshly Oiled 2	One Day after Oiling 1	One Day after Oiling 2
1-SP-30°	15.8	16.1	16.3	12.5	11.8	13.2	13.6
2-SP-30°	12.8	13.4	14.1	9.0	8.8	9.0	9.9
0-SP-90°	29.9	31.2	34.8	29.3*	32.0*	34.1*	34.9*
1-SP-90°	29.1	33.3	35.8	27.0	30.2	33.5	34.0
2-SP-90°	28.8	28.1	32.0	21.2	25.5	29.5	32.9
1-HD-30°	6.6	7.0	7.3	5.8	5.7	5.9	6.1
2-HD-30°	6.6	6.4	6.4	5.5	5.7	6.5	6.7
1-HD-90°	18.7	18.1	17.5	13.8	14.4	15.5	-
2-HD-90°	18.0	17.6	-	15.4	14.1	14.4	14.7
1-GD-30°	8.1	8.5	10.2	7.6	8.3	8.6	8.5
1-GD-90°	9.6	11.8	10.6	11.7	9.2	10.7	10.6
2-GD-30°	23.2	28.5	33.6	23.7	26.5	28.8	29.7
2-GD-90°	25.6	28.5	29.3	24.6	28.5	29.9	28.9

*Tendon was not lubricated in these tests.

Table 5-2 Average percent load loss due to curvature friction

Specimen	Test						
	Dry 1	Dry 2	Dry 3	Freshly Oiled 1	Freshly Oiled 2	One Day after Oiling 1	One Day after Oiling 2
1-SP-30°	14.8	15.1	15.3	11.5	10.8	12.2	12.6
2-SP-30°	12.3	12.9	13.6	8.5	8.3	8.5	9.4
0-SP-90°	29.4	30.7	34.3	28.8*	31.5*	33.6*	34.4*
1-SP-90°	28.1	32.3	34.8	26.0	29.2	32.5	33.0
2-SP-90°	28.3	27.6	31.5	20.7	25.0	29.0	32.4
1-HD-30°	6.1	6.5	6.8	5.3	5.2	5.4	5.6
2-HD-30°	6.1	5.9	5.9	5.0	5.2	6.0	6.2
1-HD-90°	18.2	17.6	17.0	13.3	13.9	15.0	-
2-HD-90°	17.5	17.1	-	14.9	13.6	13.9	14.2
1-GD-30°	7.6	8.0	9.7	7.1	7.8	8.1	8.0
2-GD-30°	9.1	11.3	10.1	11.2	8.7	10.2	10.1
1-GD-90°	22.7	28.0	33.1	23.2	26.0	28.3	29.2
2-GD-90°	25.1	28.0	28.8	24.1	28.0	29.4	28.4

*Tendon was not lubricated in these tests.

So far the results from the tests have been presented as the percent load loss from the live end to the dead end. However, another way of presenting the same data is in friction coefficients. The curvature friction coefficients obtained for each test is shown in Table 5-3. Table 5-2 and Table 5-3 present the same information in different ways. To obtain the friction coefficient from the percent load loss, the following procedure is used:

$$\text{Live End Load} = P_A$$

$$\text{Dead End Load} = P_B$$

$$\text{Percent Load Loss} = PL$$

$$\text{Angle Change} = \alpha$$

$$\text{Friction Coefficient} = \mu$$

$$PL = \frac{P_A - P_B}{P_A} = 1 - \frac{P_B}{P_A}$$

$$\frac{P_B}{P_A} = 1 - PL$$

$$P_B = P_A e^{-\mu\alpha}$$

$$\frac{P_B}{P_A} = e^{-\mu\alpha}$$

$$\ln\left(\frac{P_B}{P_A}\right) = -\mu\alpha$$

$$\ln(1 - PL) = -\mu\alpha$$

$$\mu = \frac{-1}{\alpha} \ln(1 - PL)$$

Table 5-3 Average Friction Coefficient

Specimen	Test						
	Dry 1	Dry 2	Dry 3	Freshly Oiled 1	Freshly Oiled 2	One Day after Oiling 1	One Day after Oiling 2
1-SP-30°	0.306	0.313	0.316	0.232	0.218	0.248	0.257
2-SP-30°	0.250	0.264	0.280	0.171	0.166	0.170	0.189
0-SP-90°	0.222	0.234	0.267	0.216*	0.241*	0.260*	0.268*
1-SP-90°	0.210	0.248	0.273	0.192	0.220	0.250	0.255
2-SP-90°	0.212	0.206	0.241	0.148	0.184	0.218	0.249
1-HD-30°	0.119	0.129	0.135	0.105	0.102	0.106	0.110
2-HD-30°	0.120	0.116	0.116	0.097	0.102	0.119	0.122
1-HD-90°	0.128	0.123	0.118	0.091	0.096	0.104	-
2-HD-90°	0.123	0.120	-	0.102	0.093	0.096	0.097
1-GD-30°	0.151	0.160	0.195	0.141	0.156	0.162	0.160
2-GD-30°	0.182	0.229	0.203	0.226	0.175	0.206	0.204
1-GD-90°	0.164	0.209	0.256	0.168	0.192	0.212	0.220
2-GD-90°	0.184	0.209	0.216	0.176	0.209	0.222	0.213

*Tendon was not lubricated in these tests.

5.2 THE EFFECT OF CURVATURE AND DUCT MATERIAL

The results of all dry tests taken from Table 5-2 (load loss) and Table 5-3 (friction coefficient) are shown graphically in Figure 5-1 and Figure 5-2, respectively. The labels on the horizontal axis specify the specimen in which the dry test was performed. For example, the leftmost bar is the result from the first dry tests on specimen 1-SP-30°, while the rightmost bar is the result from the third dry test on specimen 2-GD-90°.

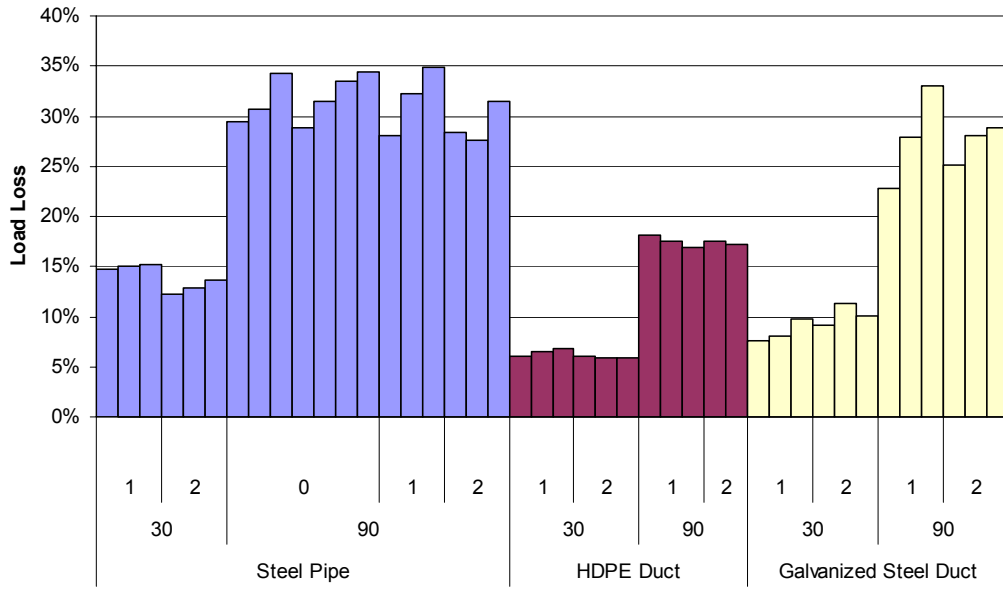


Figure 5-1 Load loss due to curvature friction on Dry tests

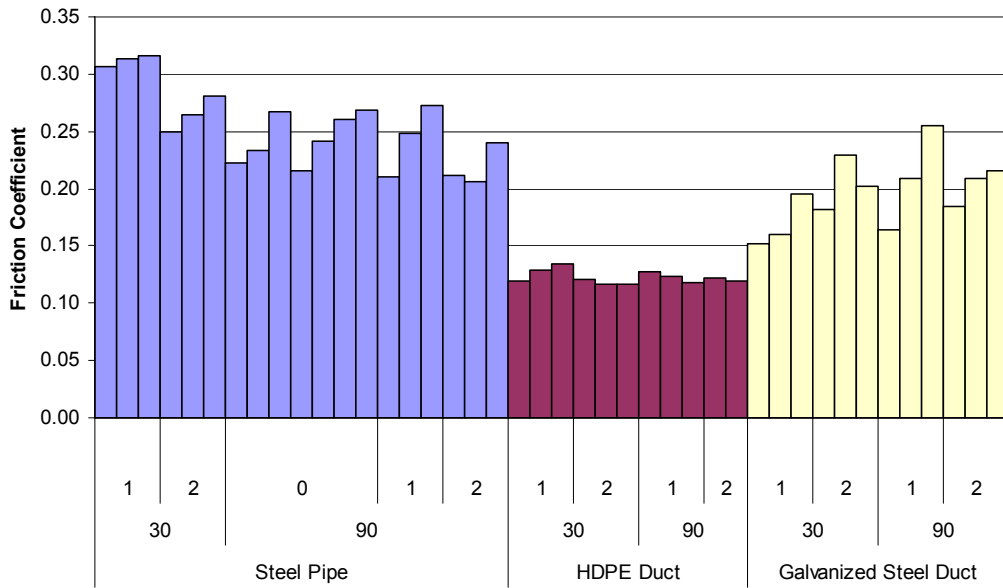


Figure 5-2 Friction Coefficients on Dry tests

The results shown in Figure 5-1 may be further summarized by taking the average of all the dry tests for a given combination of duct material and radius of curvature. The average values are shown in Figure 5-3. Figure 5-3 also shows the maximum and minimum observed value for every combination. Following the same procedure, the results from Figure 5-2 are summarized in Figure 5-4. In addition, the average value from the two radii for each duct material is shown in Figure 5-4.

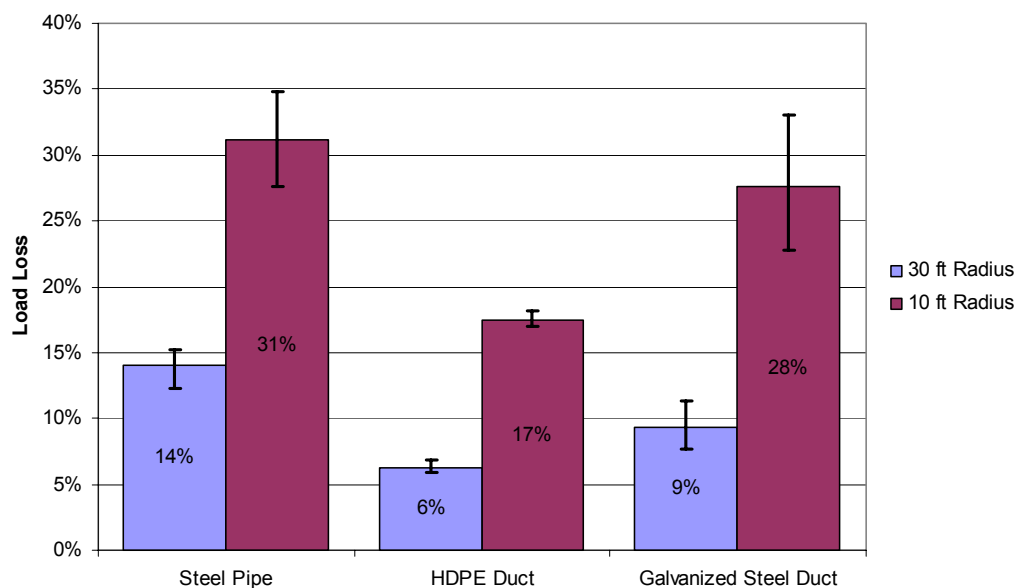


Figure 5-3 Average load loss on Dry tests

One of the secondary objectives of this study is to determine the effect of curvature on friction losses. In all cases shown in Figure 5-3, the friction losses were considerably higher for tighter curvatures. However, this is what the formula for friction losses would predict. The question is whether the coefficient of friction is dependent on the curvature. The answer lies in Figure 5-4. On specimens that used steel pipes, the coefficient of friction is lower in tighter curvature, while in specimens with galvanized steel ducts, the coefficient is higher

in tighter curvature. The two results show opposite trends, and in both cases, the differences are small relative to the scatter in the data. In addition, specimens that used HDPE ducts show little scatter, and virtually no difference in the coefficient of friction between the specimens with different curvatures. Therefore it may be concluded that the coefficient of friction is essentially independent of the radius of curvature.

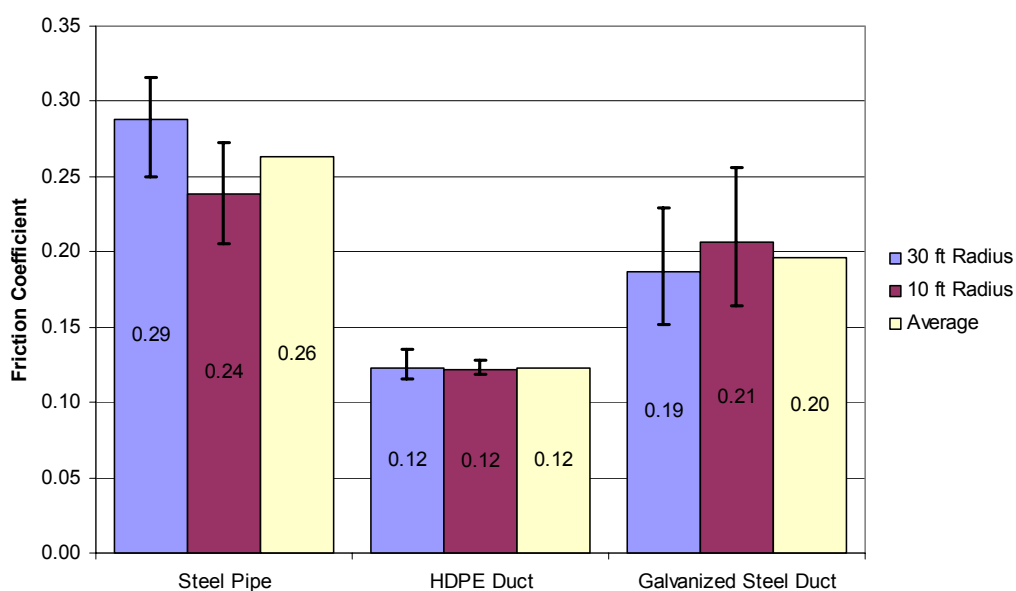


Figure 5-4 Average friction coefficients on Dry tests

Figure 5-4 also shows the effect that the duct material has on the coefficient of friction. Using galvanized steel duct as a reference, the coefficient for HDPE ducts is 40% lower, while the coefficient is 30% higher for steel pipes.

5.3 THE EFFECT OF LUBRICATION

In order to study the effect of lubrication, the average coefficient of friction from the three *Dry* tests for each specimen was compared to the average of the two *Freshly Oiled* tests and the average of the two *One Day After Oiling*

tests. The results are shown in Figure 5-5 for the *Freshly Oiled* and in Figure 5-6 for the *One Day After Oiling* tests. The figures show the reduction in the friction coefficient in each specimen due to lubrication using both oils.

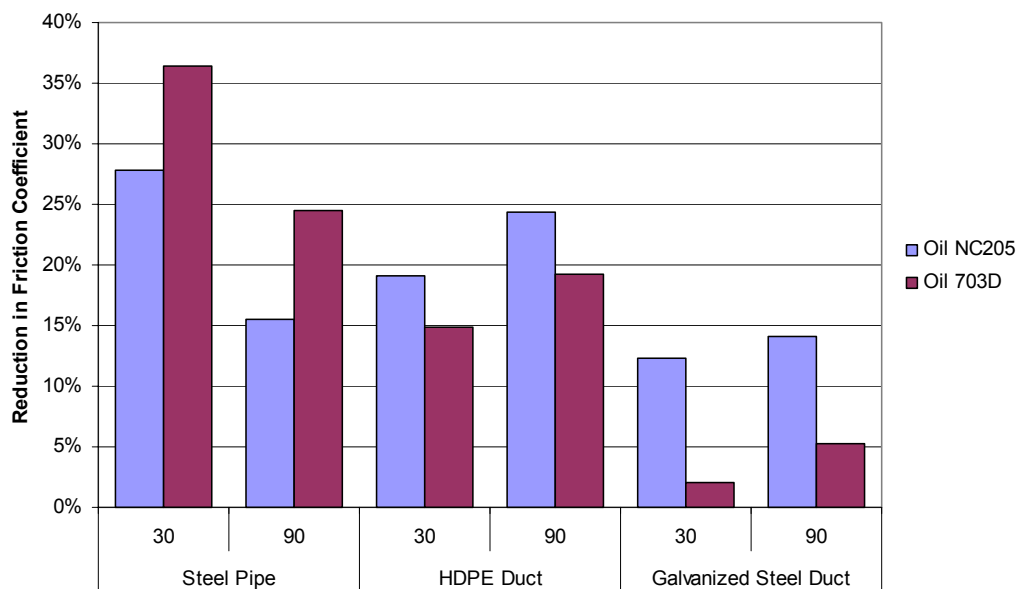


Figure 5-5 Effect of fresh lubrication

Reduction in the friction coefficient due to lubrication using oil NC205 varies from 12% to 28% and averages 19%. Reduction with oil 703D varies from 2% to 36% and averages 17%. Although the average reduction from both oils are similar, oil NC205 shows more consistent reductions. No clear trends are visible as far as the effect of curvature on lubrication. Although there is some scatter in the data from the *Freshly Oiled* tests, lubrication of tendons appears to reduce friction but it is more effective in steel pipes and HDPE ducts.

The data from the *One Day After Oiling* tests, shown in Figure 5-6, shows even more scatter. Some tests show higher coefficient of friction in the *One Day After Oiling* tests than in the *Dry* tests (shown as negative reduction). No clear trends appear from the figure. However, oil NC205 had positive reductions in four

out of six *One Day After Oiling* tests, while oil 703D only had positive reductions in two out of six tests.

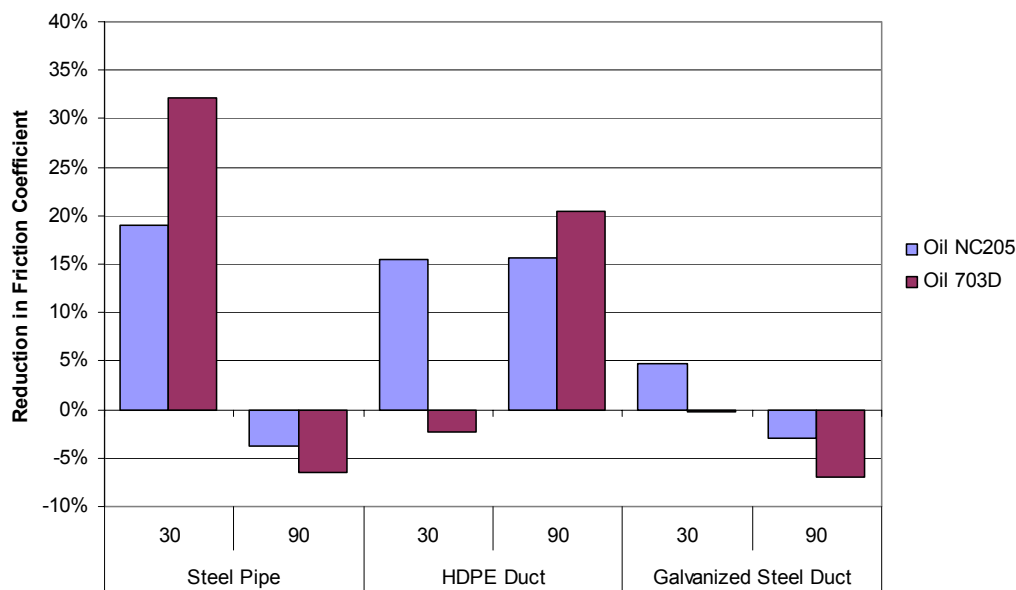


Figure 5-6 Effect of lubrication one day after oiling

Figure 5-7 compares the reduction in the friction coefficient for the *Freshly Oiled* and *One Day After Oiling* tests. All tests, with the exception of specimen 2-HD-90° (oil 703D), show decreased reductions in friction coefficients due to the one day delay in stressing of the tendon. If we consider reduction of 5% or less to be insignificant, then half of the tests in oil NC205 show no reductions in friction coefficients in the *One Day After Oiling* tests. In oil 703D two thirds of the tests show no reductions. Although in both oils tests show that the reductions in friction losses are either completely lost or significantly reduced by the one day delay, oil NC205 had better performance when compared to oil 703D. In oil NC205 only two tests show negative reductions, while oil 703D four tests do.

The effect of waiting one day after lubrication is probably dependent on other factors that were not carefully controlled on these tests. The oils dry with time, and it is believed that their effectiveness in reducing friction decreases. However, other factors such as the rate at which the oils dry and the effect of ambient condition such as temperature and humidity are all unknown. In addition, different oils are affected differently by these factors. The information available from these tests indicates that, in time, lubrication from the oils is eventually lost; however, more research is needed to establish how quickly and under what circumstances the lubricating effect is lost.

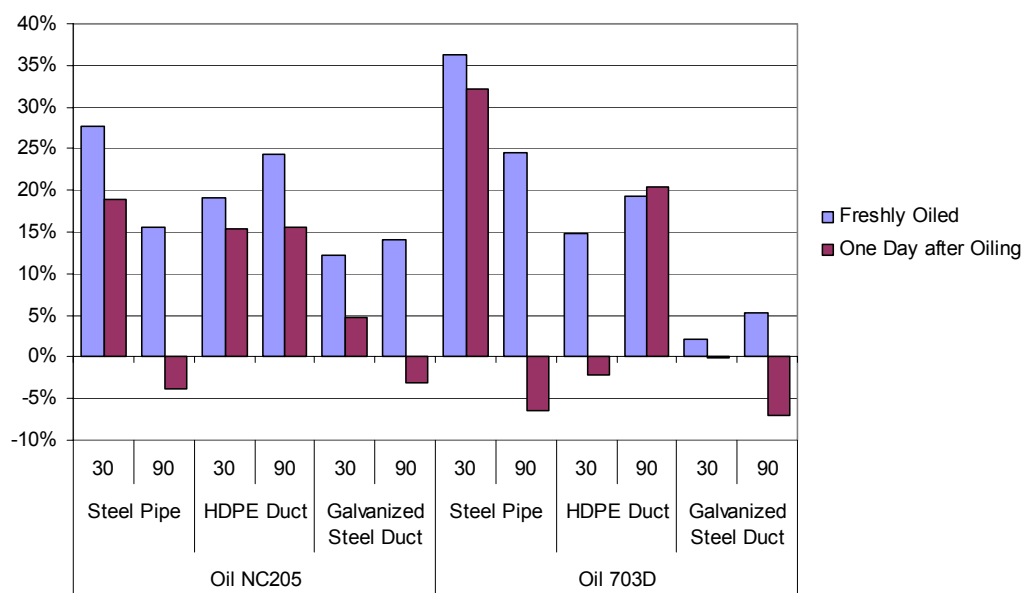


Figure 5-7 Results from Freshly Oiled and One Day After Oiling tests

5.4 COMPARISON TO DESIGN VALUES AND RECOMMENDATIONS

The average friction coefficients obtained from the *Dry* tests are 0.26, 0.12, and 0.20 for steel pipes, HDPE ducts, and galvanized steel ducts, respectively. These values are compared to those recommended for design and

those found in previous research in Table 5-4. These values have been taken from the literature review presented in Chapter 2.

The values obtained for galvanized steel ducts agree with those recommended and those found in previous research. This is expected since most of the available research and experience has been with this type of duct. Although the only available value for friction coefficients in steel ducts comes from AASHTO, it agrees with the one obtained in this research. Less research and experience is available on HDPE ducts, where more discrepancy is found between this research and other values. AASHTO’s recommended value seems high, almost twice that found in this study, and about 30% higher than that reported in NCHRP Project 4-15.

Table 5-4 Comparison of friction coefficients to recommended values

	Steel Pipe	HDPE Duct	Galvanized Metal Duct
ACI	-	-	0.16 – 0.24 (0.20 ^a)
AASHTO	0.25 ^b	0.23	0.15 – 0.25 ^c
PTI	-	-	0.15 – 0.25
NCHRP Project 4-15	-	0.18	0.23
Current Research	0.26	0.12	0.20
^a Recommended for design. ^b Lubrication will probably be required. ^c A friction coefficient of 0.25 is appropriate for 12-strand tendons. A lower coefficient may be used for larger tendon and duct sizes.			

Data from this research indicate that a conservative estimate of the coefficient of friction for HDPE ducts can be taken as 0.15. The recommended values for the coefficients in steel pipes (0.25) and for galvanized steel ducts (0.20) appear to be adequate.

No friction tests have been previously reported using the two oils that were used in this research. However, the average reduction in the friction coefficient is similar to the ones reported in previous research. The results from this and previous research are shown in Table 5-5. Results vary from no reduction

to 25%, but most of the values range between 14% and 21%, included the ones from this research. Out of the 18 reported tests only five are below 14% reduction. Therefore a reduction of 15% in the coefficient of friction due to lubrication is conservatively recommended when the actual oils are approved for use after demonstrating reduction in the friction coefficient of at least 14% in tests similar to those referenced in Table 5-5.

Table 5-5 Reduction in friction coefficients compared to previous research

		Oil	Reduction in Friction Coefficient
Owen and Moore			No Reduction
TxDOT Project 1264	Small Scale	Visconorust 8415E	17%
		Dromus B	17%
		Unocal 10	14%
		Unocal MS	14%
		Texaco Soluble D	27%
		Rust-veto FB20	0%
		Hocut 737	-9%
		Hocut 4284	18%
		Nalco 6667	12%
	Wright 502	21%	
	Large Scale	Texaco Soluble D	19%
		Wright 502 (monolithic)	25%
		Wright 502 (segmental)	15%
		Hocut 4284	17%
Dromus B		8%	
Current Research	NC205	19%	
	703D	17%	

5.5 SIGNIFICANCE OF FINDINGS

In the previous sections, the data from the tests performed in this study were analyzed and compared to the findings of previous research and to the

recommendations by ACI, AASHTO, and PTI. The objective of this section is to illustrate the practical implications of these findings. This objective will be accomplished by the use of examples.

Assume that one is to design a post-tensioned girder, and following the standard practice, galvanized steel ducts are to be used. Therefore, the assumed coefficient of friction in this case would be 0.20.

Consider the hypothetical case where the designer is trying to decide whether to use external (bonded at discrete deviators) or internal tendons, and that the total angle change and tendon length are the same for both cases. If external tendons are used then the coefficient of friction needs to be increased to 0.25 because steel pipes are used at deviators instead of galvanized steel ducts. If the designer cannot tolerate this increase in friction, he/she may use lubrication to reduce the coefficient by 15% to 0.21. In that case, the coefficient is similar to that of the galvanized steel duct.

However, if the decision has been made to use internal tendons, and the estimated friction losses are still too large, then lubrication of a galvanized steel duct will reduce the coefficient to 0.17. But if the designer decides to replace the galvanized steel ducts with HDPE ducts, instead of lubricating the tendons, then the coefficient will further drop to 0.15. Therefore, greater reduction in friction is achieved by using HDPE ducts, than by lubrication. Further reduction, to a coefficient of 0.13, is possible if both HDPE ducts and lubrication are used.

The effect of the coefficient of friction in the actual percent load loss depends on the total angle change in the tendon. The relationship between these quantities may be studied through the equation of friction loss:

$$PL = 1 - e^{-\mu\alpha}$$

This equation is presented graphically in Figure 5-8 where the coefficient of friction is plotted against percent load loss for a given total angle change. The

figure shows that for small angle changes, the percent load loss is almost independent of the coefficient of friction, in the range of practical values, whereas at high angle changes, the coefficient of friction becomes more important.

Assume that a symmetrical post-tensioned girder (half the girder is shown in Figure 5-9) is to be stressed from both ends. Half of the girder has a total angle change of 58.4 degrees. Assuming a coefficient of friction of 0.20, and a wobble coefficient of 0.0002 1/ft gives a percent load loss of 22.0% to the middle of the girder. Assuming that the tendon is stressed to 80% of its tensile capacity, the post-tensioning force at the live end is 929 kips, and 725 kips at the middle.

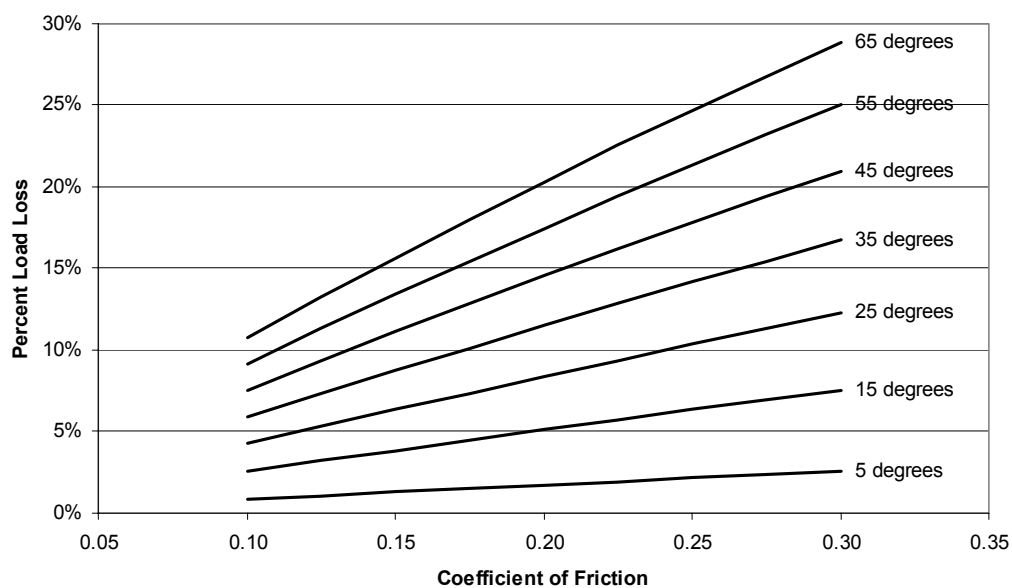


Figure 5-8 Relationship between total angle change, coefficient of friction and percent load loss

If lubrication is used, then the coefficient of friction would drop to 0.17 and the percent load loss to 19.6%. If HDPE ducts were used then the coefficient of friction would be 0.15 and the load loss 17.9%. However, a reduction of 4% in the load loss (from 22.0% loss to 17.9%) will not have a significant effect on the

design. Four percent in the area of a twenty-strand tendon is less than the area of a single strand and no strand may be removed. Therefore, reducing the coefficient of friction from 0.20 to 0.15, in this case had no effect.

However, if both HDPE ducts and lubrication are used, the coefficient of friction would be 0.128 and the load loss 16.0%. A six percent reduction in the area of a twenty-strand tendon is 1.2 times the area of a single strands. If 19 strands are used instead of 20, then the 80% of the tensile strength is 882 kips, and the load at the dead end is 741 kips. In this case the tendon force at the dead end is higher than what it was when unlubricated galvanized steel ducts were used. Saving one strand means saving 448 ft, or 302 lb of steel. A reduction of 36% in the friction coefficient leads to a reduction of five percent in the required steel area, assuming the same size strand is to be used.

Tendon: twenty 0.6 strands Grade 270

Area: 4.3 in²

Total Length: 448 ft

Wobble Coefficient: 0.0002 1/ft

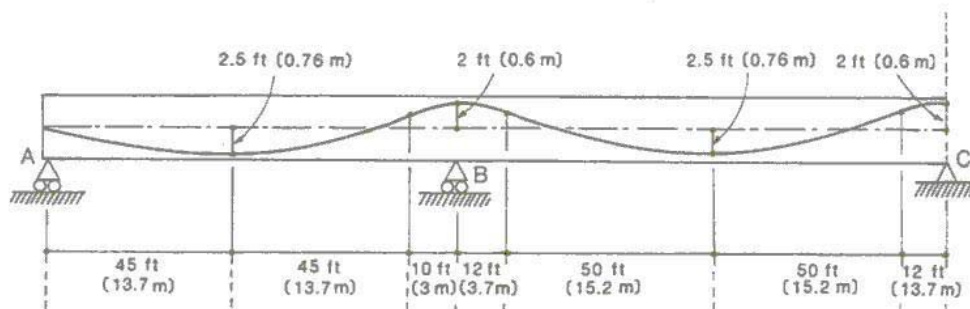


Figure 5-9 Example of friction loss calculations (Collins and Mitchell 1997)

5.6 SUMMARY

In Chapter 4 the friction loss results were presented as the load loss from the live end to the dead end as a percentage of the live end load. These were total losses. In this chapter, total loss values were first averaged for each test over the region of interest (70% to 80% of the tensile capacity of the tendon). Hardware losses were then subtracted from the average loss. Wobble losses were considered negligible. Total losses minus the hardware losses thus result in the losses due to curvature friction alone. From these curvature friction losses, average coefficients of friction were calculated.

Results from the *Dry* tests showed that the average coefficient of friction for galvanized steel duct was 0.20, for steel pipe 0.26, and for HDPE ducts 0.12. Taking galvanized steel ducts as a reference, the coefficient of friction is 30% higher for steel pipe and 40% lower for HDPE ducts. The coefficients obtained for the steel pipes and galvanized steel ducts in this research agree with the values recommended by AASHTO, ACI, PTI and with those reported in previous research. However, the coefficient of friction for HDPE ducts recommended by AASHTO is twice that found in this research and the value reported from the research of Project 4-15 is 50% higher. A value for the coefficient of friction for HDPE ducts of 0.15 is conservatively recommended for design. Analysis of the *Dry* tests also showed that the coefficient of friction is essentially independent of the radius of curvature.

Comparison of the results from the *Dry* tests to those from the *Freshly Oiled* tests showed that before drying oil NC205 on average reduced the coefficient of friction by 19%, while oil 703D reduced it by 17%. However, oil NC205 had more consistent results. Lubrication was less effective in galvanized steel ducts, especially when oil 703D was used. A reduction in the coefficient of

friction of 15% in a freshly lubricated state is conservatively recommended for design with approved oils.

Comparison of the results from the *Dry*, *Freshly Oiled*, and *One Day After Oiling* tests showed that a delay of one day after application of the oil significantly decreased or completely eliminated the reduction in the coefficient of friction due to lubrication. Although in some cases complete elimination of the reductions due to lubrication occurred in both oils, it was less frequent with oil NC205. It is recommended that no reduction in the coefficient of friction be used for design if a delay of one or more days is anticipated to occur between the application of the oil and stressing of the tendon.

Comparison of the overall performances of oils NC205 and 703D showed that they both reduced the coefficient of friction on average by approximately the same amount. However, NC205 showed more consistent results and less decrease in the reduction of the coefficient of friction due to the one day delay. Therefore oil NC205 is recommended over oil 703D.

Evaluation of the inside surfaces of the ducts after stressing, presented in Chapter 4, showed no significant damage in either the HDPE ducts or the galvanized steel ducts. AASHTO currently limits the radius of curvature for HDPE ducts to 30 ft. The limit set by AASHTO for either steel pipes or galvanized steel ducts is 10 ft. Therefore it is possible that the minimum radius of curvature for HDPE ducts could be reduced from 30 ft to 10 ft. However, this recommendation applies only when the consideration is to the damage to the inside of the duct due to stressing. Other considerations, such as the possibility of tendon breakouts on the interior face of horizontally curved members, concrete splitting and crushing from radial stresses on the inside of sharply curved tendons, and fracture of wires in sharp bends should be considered.

CHAPTER 6

Summary and Conclusions

6.1 SUMMARY

Emulsifiable oils are used to temporarily protect post-tensioning tendons from corrosion in the time between stressing and grouting. Emulsifiable oils are also used to reduce friction losses, and are expected to affect the bond strength.

The objective of TxDOT project 4562, phase one, is to investigate the use of emulsifiable oils for temporary corrosion protection, and its effects on friction, bond strength, and flexural behavior of post-tensioned members. Phase two of the project will study the use of alternate corrosion-resistant post-tensioning systems.

Phase one of the project consists of the following seven tasks:

1. Identification of emulsifiable oils
2. Accelerated corrosion testing
3. PTI/ASTM Strand pullout tests
4. Large-scale tendon friction tests
5. Large-scale bond tests
6. Development of specification and code changes
7. Preparation of reports

Tasks one through three have been completed and the results reported by Salcedo (2003). Nineteen oils were identified in task one. Both accelerated corrosion tests and PTI/ASTM Strand pullout tests were performed with these oils. Seven oils were recommended for providing adequate corrosion protection. Out of these seven oils, two were selected for the large-scale tests in tasks four and five. These oils were TRUKUT® NC205 and Nox-Rust® 703D. Oil NC205 performed the best in the pullout tests out of the seven that provide adequate

corrosion protection. It was selected to reflect the best case for the large-scale bond tests. Oil Nox-Rust® 703D performed second to last in the pullout tests, but better in the accelerated corrosion tests than the one that performed last in the pullout tests. It was selected to reflect a worst case for the large-scale bond tests. Large-scale bond tests were performed by Diephuis (2004).

Large-scale friction tests were performed using a tendon with twelve, 0.5-in. strands in three different duct materials: steel pipes, HDPE ducts, and galvanized steel ducts. Friction specimens had two different radii of curvature. Tendons were tested in three different conditions: dry, freshly oiled, and one day after oiling. Damage to the inside of the post-tensioning duct was examined.

6.2 CONCLUSIONS

The following conclusions can be made from the results of the large-scale friction tests:

1. The coefficient of friction is independent of the radius of curvature.
2. The recommended value for the coefficient of friction by ACI, AASHTO, and PTI for galvanized steel ducts is adequate.
3. The recommended value for the coefficient of friction by AASHTO for steel pipes is adequate.
4. The recommended value for the coefficient of friction by AASHTO for HPDE ducts is twice that found in this research; 0.15 is conservatively recommended for design.
5. Fresh lubrication of the post-tensioning tendon with oil TRUKUT® NC205 reduces the coefficient of friction by 19% when the oil is fresh.
6. Lubrication of the post-tensioning tendon with oil Nox-Rust® 703D reduces the coefficient of friction by 17% when the oil is fresh.

7. A reduction of 15% in the coefficient of friction due to lubrication with approved oils is recommended for design.
8. Oil TRUKUT® NC205 had overall better performance and it is therefore recommended over oil Nox-Rust® 703D.
9. No reduction in the coefficient of friction is recommended for design if stressing is to occur a day or more after lubrication.
10. No significant damage to HDPE ducts was observed, even on a radius of curvature of 10 ft, which is below the minimum allowed by AASHTO. A change on the limit in the radius of curvature of HPDE ducts is possible on the basis of damage to the inside of the duct. However, other factors should be considered before changing this limit.
11. No significant damage to the galvanized steel ducts was observed.

6.3 RECOMMENDATIONS FOR FUTURE RESEARCH

Based on the experience in testing and the data from this research, it is recommended that future research investigates whether HDPE may be safely used with radius of curvatures smaller than 30 ft.

References

1. American Association of State Highway and Transportation Officials, “Guide Specifications for Design and Construction of Segmental Concrete Bridges,” 2nd Edition, 1999.
2. American Association of State Highway and Transportation Officials, “Standard Specification for Highway Bridges,” 17th Edition, 2002.
3. American Concrete Institute Committee 318, “Building Code Requirements for Structural Concrete (ACI 318-02) and Commentary (ACI 318R-02),” 2002.
4. Carter, L. L., “Deviator behavior in externally post-tensioned bridges” Thesis, University of Texas at Austin, 1987.
5. Construction Industry Research and Information Association. “Prestressed Concrete – Friction Losses During Stressing” Report 74, 1987.
6. Collins, M. P., and Mitchell, D., “Prestressed Concrete Structures,” First Edition, 1997.
7. Cordes, H., Schütt, K., Trost, H., Großmodellversuche zur Spanngliedreibung, Deutscher Ausschuss für Stahlbeton, Berlin, 1981
8. Davis, R. T., “Friction Losses in Segmental Bridge Tendon,” Thesis, University of Texas at Austin, 1993.

9. Davis, R. T., Tran, T. T., Breen, J. E., and Frank, K. H., "Reducing Friction Losses in Monolithic and Segmental Bridge Tendons," Research Report 1264-2, Center for Transportation Research, Bureau of Engineering Research, The University of Texas at Austin, 1993.
10. Diephuis, J. R. "Factors Affecting Bond in Multi-Strand Post-Tensioning Tendons Including the Effect of Emulsifiable Oils," Thesis, University of Texas at Austin, 2004.
11. Freyermuth, C. L., "Status of the Durability of Post-Tensioning Tendons in the United States," Durability of Post-Tensioning Tendons, fib-IABSE Technical Report, Bulletin 15, Workshop 15-16 November 2001, Ghent, Belgium, 2001.
12. Hagenberger, M. J. "Consideration of Strand Fatigue for Load Rating Prestressed Concrete Bridges," Ph.D. Dissertation, University of Texas at Austin, 2004.
13. Kittleman, W. M., Davis, R. T., Hamilton, H. R., Frank, K. H., and Breen, J. E., "Evaluation of Agents for Lubrication and Temporary Corrosion Protection of Post-Tension Tendons," Research Report 1264-1, Center for Transportation Research, Bureau of Engineering Research, The University of Texas at Austin, 1993.
14. Perenchio, W. F., Fraczek, J., Pfeifer, D. W., "Corrosion Protection of Prestressing Systems in concrete Bridges," Report 313, Transportation Research Board, National Research Council, 1989.

15. Poston, R. W., and West, J. S., "North American Strategies for Improving Bonded Post-Tensioned Concrete Construction," Durability of Post-Tensioning Tendons, fib-IABSE Technical Report, Bulletin 15, Workshop 15-16 November 2001, Ghent, Belgium, 2001.
16. Post-Tensioning Institute, "Post-Tensioning Manual," Fifth Edition, 1990.
17. Salas, R. M., "Accelerated Corrosion Testing, Evaluation and Durability Design of Bonded Post-Tensioned Concrete Tendons," Ph.D. Dissertation, University of Texas at Austin, 2003.
18. Salcedo, E., "Effects of Emulsifiable Oils Used as Temporary Corrosion Protection in Grouted Post-Tensioning Tendons," Thesis, Pennsylvania State University, 2003.
19. Tran, T. T., "Reducing Friction Loss for Post-Tensioned Tendons in Monolithic Girders," Thesis, University of Texas at Austin, 1992.

VITA

Juan José Icaza Aguirre was born in Managua, Nicaragua, on October 8, 1979, the son of Elsa Olga Aguirre de Icaza and Juan José Icaza Martínez. He completed his secondary education at the American Nicaraguan School in Managua, Nicaragua, in 1997 and was admitted to The University of Texas at Austin for the fall semester of 1998. He received his Bachelor of Science in Civil Engineering in May, 2002. In August of the same year he entered the Graduate School at The University of Texas at Austin.

Permanent Address:

Apartado Postal 5003

Managua, Nicaragua

This thesis was typed by the author.